Introduction to RADAR systems

Third Edition

Merrill I. Skolnik

McGRAW-HILL INTERNATIONAL EDITIONS
Electrical Engineering Series

chapter

8

Propagation of Radar Waves

8.1 INTRODUCTION

Most of the discussion of the radar equation in Chap. 2 considered the radar energy to propagate in free space. In the real world, however, the earth's surface and atmosphere can have major effects on radar performance. In Sec. 2.12 we briefly mentioned a few of the propagation factors that can influence the range and coverage of a radar. Since propagation effects might extend the radar range significantly or reduce it drastically, it is important to account for the earth's environment when attempting to predict radar performance.

Free-space radar performance is modified by the following propagation effects:

- *Forward scattering* (reflection) of the radar energy from the surface of the earth, which enhances the radiated energy at some elevation angles and decreases it at others.
- *Refraction* (bending) of the radar energy by the earth's atmosphere, which can cause the radar energy to deviate from straight-line propagation.
- *Ducting* (trapping) of the radar energy, a form of severe refraction, which causes extended radar ranges (and, surprisingly, might not always be a good thing).
- *Diffraction* of radar waves by the earth's surface that causes energy to propagate beyond the normal radar horizon. It applies mainly at the lower frequencies that are seldom used for radar applications.

- *Attenuation* of radar waves by the clear atmosphere, which generally has little or no effect on microwave propagation.
- *External noise* that enters the radar receiver and increases the receiver noise level.
- *Backscatter from land, sea, and weather clutter, and attenuation in rain and other hydrometeors.* These are not discussed here since they were included in Chap. 7.

Most of the significant propagation effects at microwave radar frequencies occur within the line of sight of the radar. Diffraction effects when the radar is at a sufficiently low frequency, and ducting at almost any microwave frequency, can cause radar waves to bend around the surface of the earth and extend the radar range beyond the normal line-of-sight horizon.

Although the basic theory of radar propagation may be well understood, accurate quantitative predictions for a particular place and for a specific time in the future are not always easy to obtain because of the difficulty in acquiring the necessary information about the environment in which a radar operates. In some respects, predicting the effects of propagation is a little like forecasting the weather. The radar system designer is usually interested in a long-term statistical description of propagation effects so that the radar can be designed to fulfill its mission satisfactorily. Sometimes, however, the radar designer has to be content with only a qualitative knowledge of "average" propagation effects. The military tactical commander or the air-traffic controller is not as interested in the long-term statistical effects of propagation or average conditions, but is more interested in the current or short-term forecast of radar propagation conditions that might be encountered. For example, based on current measurements of the environmental factors that affect radar propagation, a military tactical planner might be able to determine a flight profile of an attacking aircraft that would minimize the range where it is first detected by a defender's radar.

8.2 FORWARD SCATTERING FROM A FLAT EARTH

To determine the type of effects the earth's surface has on radar propagation, we initially assume a plane, smooth, perfectly reflecting flat earth. The results obtained with this simplification are indicative of what is obtained with more realistic models. The geometry is shown in Fig. 8.1a. The radar antenna is located at a height h_a above the planar surface. Its antenna radiation pattern is assumed to be uniform in elevation angle. The target is at a height h_t and at a range R from the radar. The ground distance between the radar and the target is D (not shown in the figure). Energy radiated by the radar antenna arrives at the target via two separate paths. One is the direct path (AB) from radar to target; the other is the path (AMB) from the radar to the target that includes a forward-scatter reflection from the surface. The signal reflected by the target also arrives back at the radar by these same two paths. The magnitude of the resultant echo signal back at the radar antenna depends on the amplitudes and relative phases of the signals that propagate via the direct and surface-scattered paths. The modification of the field strength η (measured in volts/meter) caused by the presence of the earth's surface may be expressed by the ratio

$$\eta = \frac{\text{field strength at target in presence of earth's surface}}{\text{field strength at target if in free space}} \qquad [8.1]$$

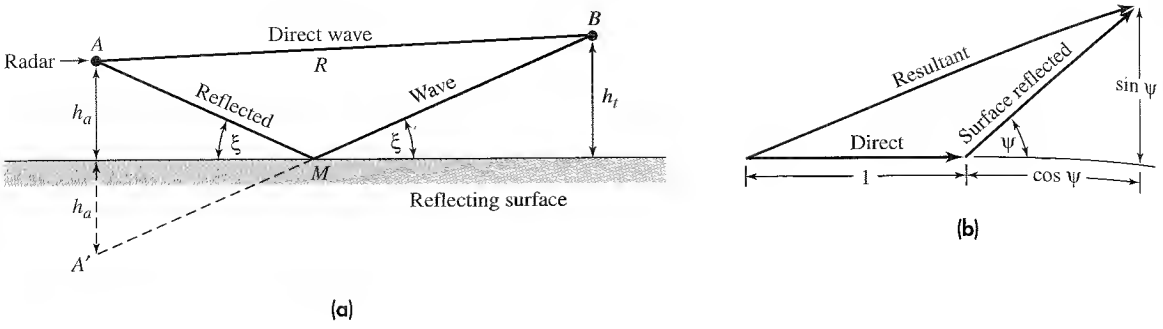

Figure 8.1 (a) Geometry illustrating radar propagation over a plane reflecting surface. (b) Vector addition of direct and surface-reflected signals, each of unity amplitude, with a phase difference of ψ.

It is assumed in this analysis that the path lengths of the direct and surface-reflected signals are almost (but not quite) equal so that the amplitudes of the two signals are essentially the same, except for any loss of signal suffered on reflection from the earth's surface. That is, if the two signals differ in amplitude from one another it is due to the surface reflection-coefficient being less than unity, and is not due to a significant difference in the $1/R^2$ factor. The slight range difference between the direct and surface-reflected paths, however, results in a difference in phase between the two which, when they combine at the target or at the radar, affects their sum. There is also a change in phase of the signal when it is reflected from the surface. This is represented by a reflection coefficient, which is a complex quantity $\Gamma = \rho e^{j\psi_r}$. The magnitude ρ describes the change in amplitude on reflection, the argument ψ_r describes the phase shift.

In this particular analysis we take the reflection coefficient to be $\Gamma = -1$. Thus the surface-reflected wave does not change its amplitude on reflection, but its phase is shifted by an amount $\psi_r = \pi$ radians. A reflection coefficient of $\Gamma = -1$ applies to a perfectly smooth, perfectly conducting surface if the radiation is horizontally polarized and the grazing angle is small.

The problem is easier to analyze if we replace the surface-reflected signal with the signal radiated from the image of the radar antenna that is below the surface, at A' in Fig. 8.1a. Instead of the surface-reflected path AMB, we consider the equivalent straight-line path $A'MB$. The path length AB is

$$AB = [D^2 + (h_t - h_a)^2]^{1/2} = D\left[1 + \frac{(h_t - h_a)^2}{D^2}\right]^{1/2}$$
$$\approx D\left[1 + \frac{1}{2} \cdot \frac{(h_t - h_a)^2}{D^2}\right] = D + \frac{(h_t - h_a)^2}{2D} \qquad [8.2]$$

In the above we assumed $|h_t - h_a| << D$. The surface-reflected path length AMB, or its equivalent, $A'MB$ is similarly

$$AMB = A'MB = [D^2 + (h_t + h_a)^2]^{1/2} \approx D + \frac{(h_t + h_a)^2}{2D} \qquad [8.3]$$

where we have assumed that $h_t + h_a << D$. Subtracting Eq. (8.2) from Eq. (8.3) results in the difference between the two paths $AMB - AB$, which is $\Delta = 2h_t h_a/D$. We make the assumption that the horizontal distance D can be replaced by the range R, so that the difference between the two paths is

$$\Delta \approx \frac{2h_a h_t}{R} \qquad [8.4]$$

To recapitulate, the geometrical assumptions we have made are that $(h_t \pm h_a) << D \approx R$. The phase lag ψ_Δ associated with this difference is found by multiplying Eq. (8.4) by $2\pi/\lambda$. The total phase difference is then

$$\psi = \psi_\Delta + \psi_r = \frac{4\pi h_a h_t}{\lambda R} + \pi \qquad [8.5]$$

At the target there are two signals, the direct and surface-reflected, which are of the same approximate amplitude with a phase difference between them of ψ, as given in Eq. (8.5). To obtain η, the vector addition of these two signals is divided by the signal amplitude that would have appeared if in free space. The value of η is found by applying the Pythagorean theorem to the sum of the two signal vectors, Fig. 8.1b, both of the same amplitude (normalized to unity) but with relative phase ψ. This gives

$$\eta = [(1 + \cos\psi)^2 + (\sin\psi)^2]^{1/2} = [2(1 + \cos\psi)]^{1/2} \qquad [8.6a]$$

The value η^2 is the ratio of the signal power density (W/m^2) at the target to the power density that would have been at the target if it were in free space, which becomes

$$\eta^2 = 2\left(1 - \cos\frac{4\pi h_a h_t}{\lambda R}\right) = 4\sin^2\left(\frac{2\pi h_a h_t}{\lambda R}\right) \qquad [8.6b]$$

Because of reciprocity in propagation, the path from target to radar is the same as that from radar to target. The echo signal power density received at the radar, relative to what would have been received in free space, is the fourth power of η, or

$$\eta^4 = 16\sin^4\left(\frac{2\pi h_a h_t}{\lambda R}\right) \qquad [8.7]$$

Lobing The radar equation describing the received echo power is multiplied by the factor η^4 as given by Eq. (8.7). Since the sine function varies from 0 to 1, the factor η^4 varies from 0 to 16. The effect of the earth's surface in this simplified example is to increase the received signal power at some elevation angles by as much as 16. At other elevation angles it can be zero. Because of the fourth-power relation between range and received echo-signal power, the radar range will vary from 0 to 2 times the range the radar would have if it were in free space. The result is that the radiation in elevation is broken up into lobes which increase the range at some elevation angles and decrease it at others, as shown in Fig. 8.2. This effect is sometimes called *lobing*.

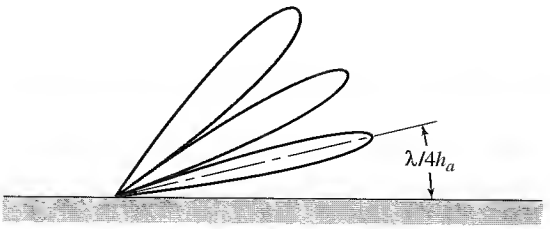

Figure 8.2 Vertical (elevatian) labe structure af the radar radiatian caused by the presence of a planar reflecting surface.

The field strength in the presence of the earth's surface is a maximum when the argument of the sine term in Eq. (8.7) is equal to $\pi/2, 3\pi/2, \ldots, (2n + 1)\pi/2$, where $n = 0, 1, 2, \ldots$. The peaks of the lobes occur when

$$\frac{4h_a h_t}{\lambda R} = 2n + 1 \qquad \text{maxima} \tag{8.8}$$

and the nulls, or minima, occur when the sine term is zero, or when

$$\frac{2h_a h_t}{\lambda R} = n \qquad \text{minima} \tag{8.9}$$

From Eq. (8.8), the angle of the peak of the first (lowest) lobe ($n = 0$), is at

$$\theta_1 \approx h_t/R = \lambda/4h_a \tag{8.10}$$

Thus if it is desired to see targets at low angles, the wavelength must be small (high frequency) and/or the antenna height must be large.

To illustrate the effects of a flat, smooth, perfectly reflecting earth's surface on radar performance we include η^4 in the simple form of the radar equation [Eq. (1.6)], which then becomes

$$P_r = \frac{P_t G^2 \lambda^2 \sigma}{(4\pi)^3 R^4} \cdot 16 \sin^4\left(\frac{2\pi h_a h_t}{\lambda R}\right) \tag{8.11a}$$

When the argument of the sine is small,

$$P_r \approx \frac{4\pi P_t G^2 \sigma (h_a h_t)^4}{\lambda^2 R^8} \tag{8.11b}$$

This represents the region below the peak of the first lobe. For targets at small angles (lower than the first lobe), the signal power is seen to vary as the inverse eighth power of the range, rather than as the inverse fourth power as occurs in free space.* The gain and wavelength appear in Eq. (8.11b) as the factor G/λ instead of $G\lambda$. The above applies for an antenna with a constant gain as a function of frequency. A different result is obtained if the effective aperture of the antenna is maintained constant with change in frequency.

*As shall be seen later, the variatian of signal strength with range at law angles can be much more complicated than that given by Eq. (8.11b), especially under canditians af anamalaus propagation.

Surface Reflection Coefficient In the above several simplifying assumptions were made. One was that the antenna elevation pattern was uniform. With an actual antenna the antenna gain as a function of elevation angle has to be taken into account since the gain in the direction of the target can be different from the gain in the direction of the surface-reflected ray. Another assumption was that the surface was smooth and perfectly reflecting. This is not always realistic since the reflection coefficient depends on the surface roughness, the dielectric properties of the surface, polarization of the radar energy, and the frequency. Figure 8.3a gives the magnitude of the reflection coefficient as a function of the grazing angle and frequency for vertical polarization over smooth sea water. Figure 8.3b is the phase of the reflection coefficient for vertical polarization and a smooth sea. The magnitude of the reflection coefficient for horizontal polarization is given in Fig. 8.3c. The phase of the reflection coefficient for horizontal polarization is approximately

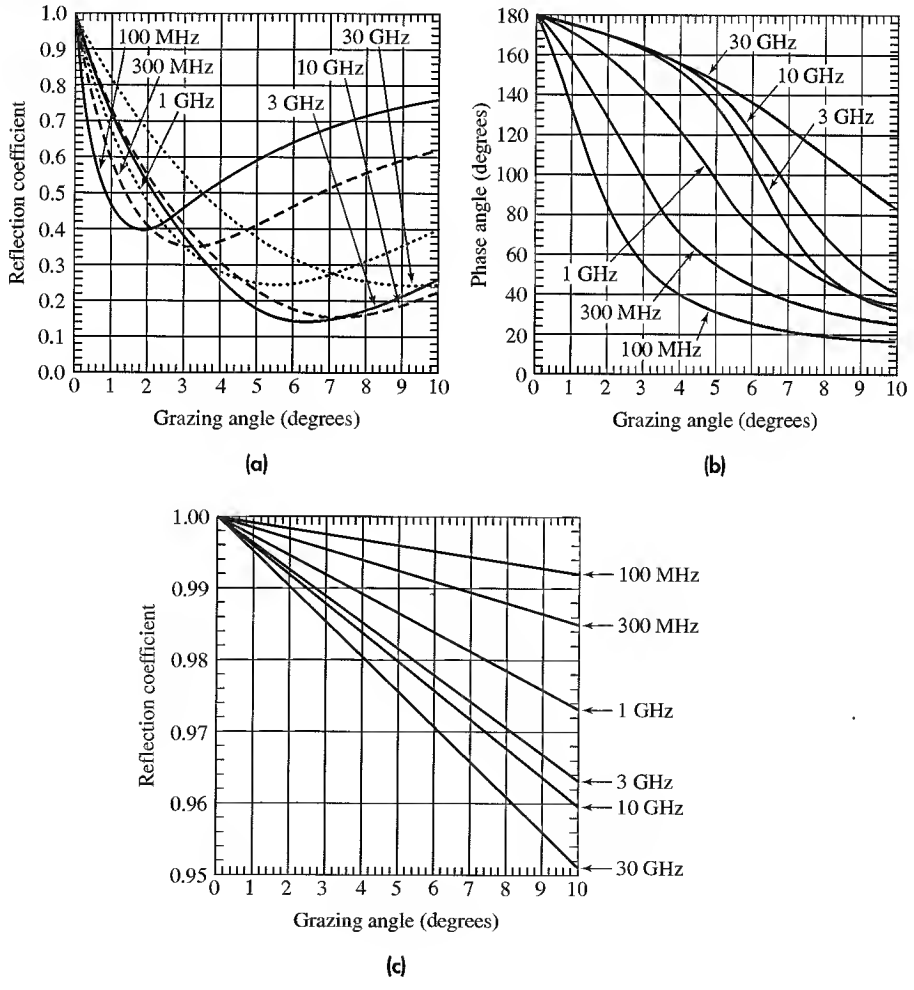

Figure 8.3 Reflection coefficient for a smooth sea as a function of grazing angle, frequency, and polarization. (a) Magnitude of the reflection coefficient for vertical polarization; (b) phase of the reflection coefficient for vertical polarization (phase of the reflected wave lags the phase of the incident wave); (c) magnitude of the reflection coefficient for horizontal polarization. The phase of the reflection coefficient for horizontal polarization is 180°, and is approximately independent of grazing angle and frequency. (From Lamont Blake, *Radar Handbook.*[20])

π radians, and doesn't vary much with frequency or grazing angle. The magnitude of the reflection coefficient is generally less for vertical polarization than for horizontal.

The minimum reflection coefficient for vertical polarization occurs at a grazing angle known as the *Brewster's angle.* When the reflection coefficient is less than unity and/or the phase of the surface reflection is not 180°, the nulls in the radiation pattern due to multipath will not be as deep and the peak value of the various lobes will decrease.

Surface roughness depends on the physical roughness *relative* to the radar wavelength. The lower the radar frequency (longer the wavelength), the smoother a surface will appear to the radar and the more likely the lobing pattern due to multipath will be highly pronounced. For example, the range in the direction of the lowest lobe of a VHF radar that is suitably sited over a sea surface might be increased almost by the theoretical factor of two indicated by the simple flat-earth model. At the higher microwave and millimeter wave frequencies, the less pronounced will be the effects of lobing.

The different values of reflection coefficients shown in Fig. 8.3 for vertical and horizontal polarization can result is different coverage patterns. The nulls with vertical polarization are not as deep and the maxima are not as great as with horizontal polarization. Vertical polarization might be specified when more uniform vertical coverage is desired and horizontal polarization might be preferred when greater range in the direction of the lobes is more important than more uniform coverage. Almost all air-surveillance radars, however, seem to employ horizontal polarization. The greater range at some elevation angles is a benefit that many radar manufacturers take advantage of when advertising the capabilities of their radars. The fact that there also are holes in the "long range" coverage with horizontal polarization is seldom deliberately mentioned.

Rough Surface Reflection Coefficient The theoretical curves of Fig. 8.3 assume a smooth reflecting surface. A smooth surface is sometimes defined by the *Rayleigh roughness criterion* which considers a surface to be smooth if $h \sin \psi < \lambda/8$, where ψ is the grazing angle and h is the difference between the extremes of the surface height. (Some take h to be approximately $4\sigma_h$, and some take it to be $3\sigma_h$, where σ_h is the standard deviation of the gaussian distribution of the surface heights.) A surface is smooth or rough to a radar signal depending on the grazing angle and the physical roughness relative to the radar wavelength.

The surface roughness can affect the reflection coefficient more than the electrical properties of the surface which enter into the reflection coefficients given by Fig. 8.3. Measurements by many workers have shown that the reflection coefficient for normal (nonsmooth) ground terrain is in the range 0.2 to 0.4 and is seldom greater than 0.5 at frequencies above 1500 MHz at low grazing angles.[1] An expression for the reflection coefficient ρ_r of a rough, perfectly conducting surface, such as the sea, was originally given by Ament[2] as

$$\rho_r = \rho_0 \exp\left[-2k^2\overline{h^2} \sin^2 \psi\right] \qquad [8.12]$$

where ρ_0 is the complex reflection coefficient for a smooth surface (Fig. 8.3), $k = 2\pi/\lambda$, λ = wavelength, $\overline{h^2}$ is the mean square surface height, ψ is the grazing angle, and h has a mean value of zero. Experimental data taken over the sea fit the expression of Eq. (8.12) for small values of the *surface roughness parameter* defined as $(\sigma_h \sin \psi)/\lambda$, where σ_h is the rms value of the surface height h. The Ament theory underestimates the experimental

data of Beard[3] when the roughness parameter is greater than 0.1. Miller, Brown, and Vegh[4,5] extended the theoretical analysis of Ament and obtained the following expression for the rough-surface reflection coefficient

$$\rho_r = \rho_0 \exp\left[-2k^2\overline{h^2}\sin^2\psi\right] \cdot I_0(k^2\overline{h^2}\sin^2\psi) \qquad [8.13]$$

where $I_0(z)$ is the modified Bessel function of zero order. Eq. (8.13) is Ament's equation multiplied by the I_0 factor. It fits experimental data for roughness parameters less than 0.3. Figure 8.4 plots Ament's expression along with its modification, Eq. (8.13), and a set of experimental data.

In the above the *specular,* or *coherent,* component of the scattered signal has been discussed. There is also a *diffuse,* or *incoherent,* component of reflection.[6] Its phase and amplitude are random, and scattering occurs over a wider range of angles than does the specular component. It has been reported to increase linearly with increasing surface roughness parameter, level off to a maximum, and then decrease as the inverse square root of the roughness parameter.

The surface-scattered energy that causes lobing of the antenna elevation pattern not only affects the coverage of a radar but it also can introduce serious errors in height-finding methods as well as degrade low-angle tracking (as was discussed in Sec. 4.5).

The effect of the surface-scattered wave on the coverage of the radar is indicated in the radar equation by the propagation factor F^4, where F is defined as

$$F = \frac{E_s}{E_0} \qquad [8.14]$$

where E_s is the field strength of the signal at the target (it includes the effects of the antenna pattern normalized to unity gain), and E_0 is the electric field strength that would occur in free space with loss-free isotropic antennas. It is similar to the parameter η defined by Eq. (8.1) except that F includes the effects of the antenna pattern on the elevation coverage. The propagation factor F was included in the numerator of the radar equation given in Chap. 2 as Eq. (2.61)

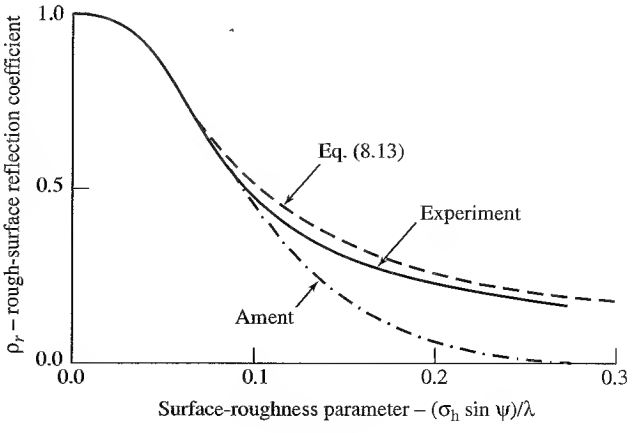

Figure 8.4 Surface reflectian coefficient ρ_r as a functian af the surface raughness parameter defined as $(\sigma_h \sin \psi)/\lambda$, where σ_h = rms value af the surface height h, ψ = grazing angle, and λ = radar wavelength. Tap curve is the thearetical expressian given by Eq. (8.13), battam curve is the original expressian given by Ament as in Eq. (8.12), and the middle curve is the experimental data af Beard. (After A. R. Miller and E. Vegh, Naval Research Laboratory Report 8898, July 31, 1985.)

8.3 SCATTERING FROM THE ROUND EARTH'S SURFACE

The use of a flat-earth model is quite suitable for understanding the general nature of the modifications that occur in the antenna coverage. The earth, of course, is not flat, and precise predictions of the effect of the surface on the antenna coverage must consider the round earth. This is especially true for coverage at low elevation angles near the horizon.

The reflection coefficient from a round earth is less than from a flat-earth surface because of the divergence, or widening, of the beam when scattered from a round surface. The so-called *divergence factor* describes the decrease in the scattered signal. The divergence of the beam, however, means that the reflected energy will be spread over a wider angular region than specular scattering from a flat surface. The grazing angle of specular reflection is easy to determine for a perfectly flat surface, but this same angle from a spherical surface is more difficult to compute. In the past it has been found using either approximations or numerical computations; but Miller and Vegh have provided a deterministic method for obtaining the grazing angle from a spherical surface.[7]

There exists in the literature the necessary information, graphs, and nomographs to compute the coverage of a radar when lobing occurs due to the presence of the earth's surface.[8,9] This can be tedious when done by hand, especially when there are many lobes generated in the coverage. Computer programs are available that considerably ease the burden of calculating and plotting the coverages, one of the first of which was by Lamont Blake.[10]

An example of a calculated coverage diagram for an *L*-band radar over sea water is shown in Fig. 8.5 for both horizontal and vertical polarization. At low angles the maximum range with vertical polarization in this example is decreased only slightly relative to the range with horizontal polarization. The effect of the Brewster angle on vertical polarization, however, can be seen in the reduced ranges at higher elevation angles. One of the major consequences of the lobed elevation pattern due to multipath is that tracking of an aircraft flying at a constant altitude will not be continuous. Echoes will be received when the target is in one of the lobes, but the target might not be detected when it is in a null between the lobes. For instance, a target flying at a constant height of 30,000 ft will first be seen by a radar, whose coverage pattern is given by Fig. 8.5a, at a range of 170 nmi. The target will be lost at 160 nmi, reappear at 146 nmi, be lost again at 136 nmi, and so forth. The coming and going of the radar echo can create problems with automatic detection and tracking systems. In such systems, allowance has to be made for the track to coast whenever the target is momentarily lost, rather than immediately drop the track as soon as it leaves the coverage of a lobe and have to initiate a new track when the target echo reappears.

As has been mentioned, the effect of the interference between the direct and surface-scattered waves is to cause the peak of the lowest lobe of the elevation coverage to be at an angle higher than zero degrees, as was seen by Eq. (8.10) for the example of a flat earth. The lowest lobe with a round earth likewise will be at some angle above the horizontal. The result will be a lack of coverage of low-altitude targets. Figure 8.6a is a sketch of the elevation coverage of a long-range enroute air-traffic control radar. The details of the lobing are not shown. (There are two beams, an upper and a lower. We need only be

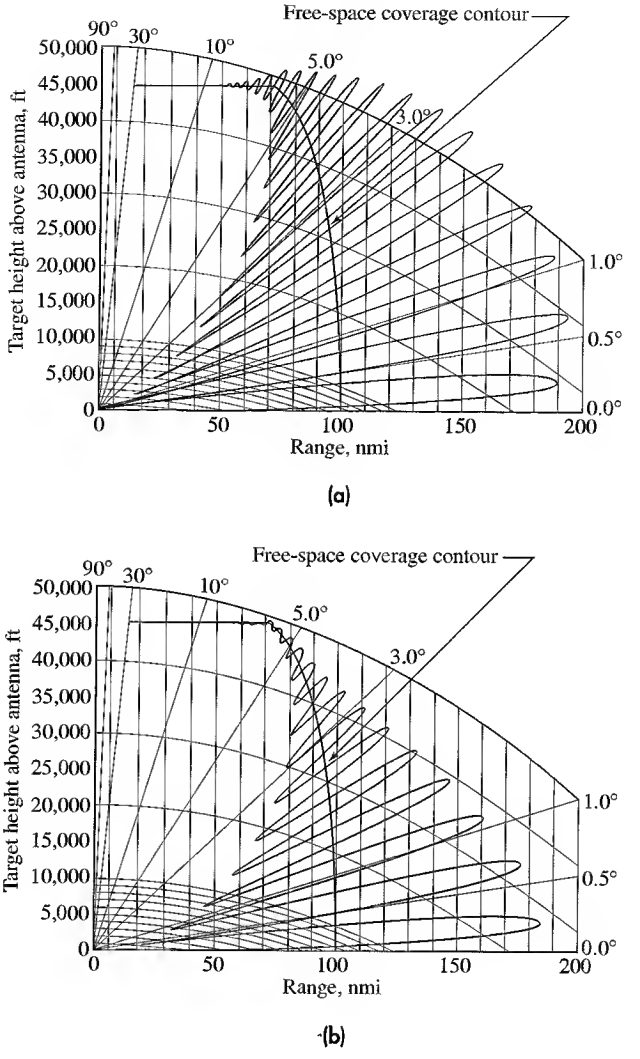

Figure 8.5 Example of a calculated vertical-plane coverage diagram for (a) horizontal polarization and (b) vertical polarization. Frequency = 1300 MHz, antenna height = 50 ft, antenna vertical beamwidth = 12° with the beam maximum pointing on the horizon, a sea surface with 4 ft wave height and free-space radar range of 100 nmi.

concerned with the lower.) The lower beam is tilted so that its half-power point, rather than its maximum, is on the horizon. This makes the lobes (which are not shown) less pronounced, but it also decreases the coverage at low altitudes. The radar is seen to have a maximum range of about 235 nmi. This is a good range for an air-surveillance radar, until it is noted that this range occurs at an altitude in the vicinity of 85,000 ft, which is much higher than commercial aircraft fly. The range for an aircraft flying at 30,000 ft, according to this coverage diagram, is about 185 nmi, and is 165 nmi when the altitude

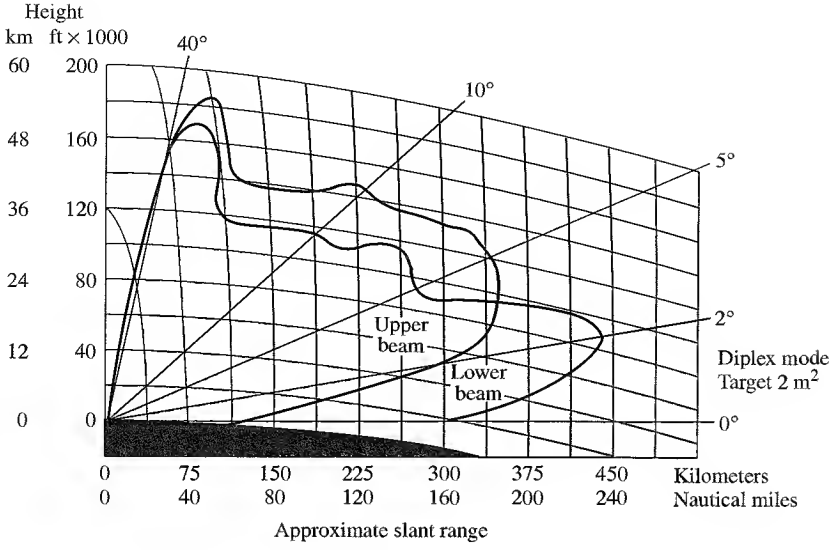

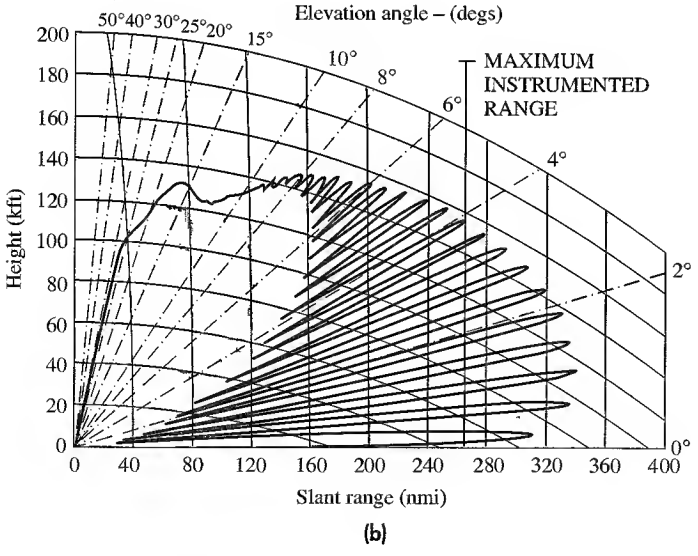

Figure 8.6 (a) Vertical coverage diagram of an *L*-band long-range en-route air-traffic control radar, illustrating the reduced range of the lower beam at very low angles due to the multipath from the earth's surface. (From the brochure *The ARSR-3 Story,* Westinghouse Defense and Electronic System Center, Baltimore, MD. Courtesy of Northrup Grumman Corporation.) (b) Calculated vertical coverage diagram of the Raytheon AN/SPS-49 radar. Long-range mode with antenna rotation rate of 6 rpm, 0.50 probability of detection, 10^{-6} probability of false alarm, Swerling Case 1 target with 1 m^2 radar cross section, sea state 3, and antenna height of 75 ft. This radar operates in the band from 850 to 942 MHz, with an antenna gain of 29 dB and an average transmitter power of 13 kW. (Courtesy of Vilhem Gregers-Hansen and the Raytheon Co.)

is 20,000 ft. Thus the quoted range of a radar might be much greater than the actual range at which an aircraft is first detected when flying at its more usual altitudes. If low-altitude performance at long range is important, the radar should be located on high ground so that its first lobe will be lowered in angle.

Another example of radar coverage, shown in Fig. 8.6b, is that of a long-range shipboard air-surveillance radar known as the AN/SPS-49.

Methods for Minimizing Lobing Effects In many instances, the added range produced by the multipath lobing is a desirable attribute in spite of the nulls which can cause loss of targets. In other cases, lobing might not be desired. This can be true for automatic tracking radars or when the target undertakes maneuvers that require the radar to obtain information at a high data rate. One method to reduce the effects of lobing is to tilt the antenna beam upward so that the radiated energy illuminating the surface is reduced. Thus it is customary in many air-surveillance radars to tilt the beam so that its lower half-power point lies on the horizon.

We have seen that the location of multipath nulls depends on the frequency and the antenna height. By changing the height of the antenna (switching the radar between antennas at different heights) or by changing the radar frequency, the nulls can be filled-in when the radar data from the two or more antennas at different heights are combined. The utility of *height diversity* is limited by the need for antennas at different heights and by the difficulty in obtaining more than two different heights. *Frequency diversity* has been demonstrated to effectively fill in the nulls and allow continuous tracking of the target.[11] This capability, however, requires a wide frequency band. A wide frequency range is highly desired in many applications since it has other advantages than just filling in the nulls.

A radar with *polarization diversity* utilizes two orthogonal polarizations, such as horizontal and vertical. It could, in principle, provide some filling in of the nulls, but it has seldom been used. The nature of the Brewster's angle seems to limit its utility.

A *fence* surrounding the radar antenna can prevent radiated energy from illuminating the ground and can thus reduce lobing. This has seldom been employed since a fence can be large and expensive, diffraction from the edge of the fence limits the amount of attenuation of ground clutter that can be achieved, and there can be a loss of detection of desired low altitude targets.

The land-based military air-surveillance radars used in World War II did not employ doppler processing for separating the unwanted clutter from the doppler-shifted echoes from moving targets. For this reason, when conditions allowed, the radars were sited where there might be natural shielding to attenuate the energy radiated in the direction of the surface. Modern military radars, however, have to see targets at low altitude and would not benefit from this technique.

Not much can be done to enhance the signals from targets that lie below the first lobe. This is why surface-based radars that might have large free-space ranges have significantly reduced detection ranges against targets low on the horizon.

The lobing effect was put to good use in World War II for obtaining the height of an aircraft by using VHF radars that were capable of measuring only azimuth angle and not elevation angle. The range of first detection seen by the lowest lobe was used as an indication of target height. This required good calibration of the radar's sensitivity, and

calibration flights with known aircraft to verify the relation between aircraft height and range of first detection. It also required the enemy to cooperate by not introducing new aircraft whose echo signals might be of quite different strength than those on which the radar was calibrated. In spite of its limitations, this method of height finding did what was required at the time.

8.4 ATMOSPHERIC REFRACTION—STANDARD PROPAGATION

Radar waves travel in straight lines in free space. Propagation in the earth's atmosphere, however, is not in free space. The atmosphere is not uniform; hence, it causes electromagnetic waves to be bent, or refracted. Normally the effect of bending caused by atmospheric refraction is favorable, in that it causes the radar horizon to be extended and increases the coverage of a radar beyond the geometrical horizon, Fig. 8.7a. On the other hand, the bending of the rays by the atmosphere can introduce an error in the measurement of the elevation angle, Fig. 8.7b.

Refractivity Refraction of radar waves in the atmosphere is due to the variation of the velocity of propagation with altitude. The *index of refraction* is a measure of the velocity of propagation and is defined as the velocity in free space divided by the velocity in the medium in question, the atmosphere in this case. (The index of refraction is the square root of the dielectric constant, a parameter that might be more familiar to the electrical engineer.) The difference in velocity of propagation in the atmosphere compared to that

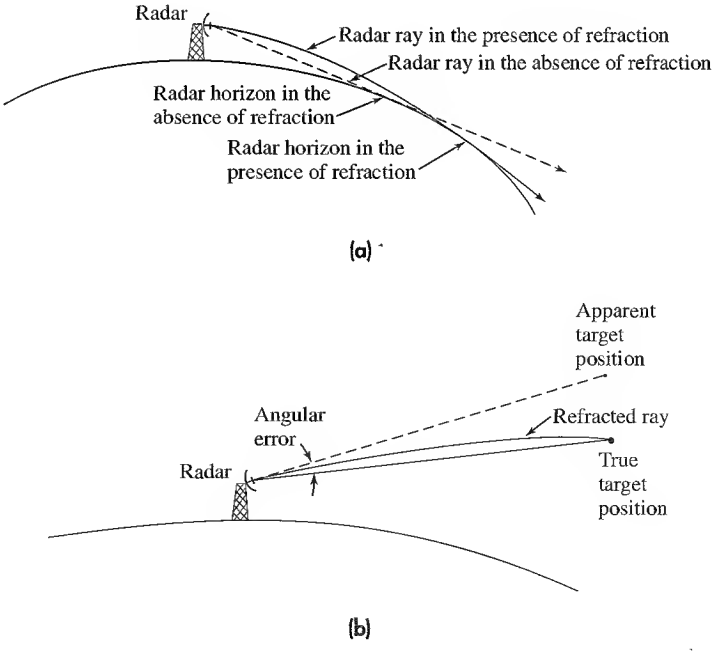

Figure 8.7 (a) Extension of the radar horizon due to refraction of radar rays by the atmosphere; (b) angular error caused by atmospheric refraction.

in free space is very small. According to the International Telecommunications Union, the average value of the surface index of refraction at mid-latitudes is 1.000315.[12] (Hitney,[13] on the other hand, gives 1.000350 as a typical value for the index of refraction at the earth's surface.) Rather than use the index of refraction, n, it is more convenient to use a modified parameter called the *refractivity, N,* which is defined as $N = (n - 1)10^6$. Thus an index of refraction $n = 1.000315$ corresponds to a refractivity $N = 315$.

At microwave frequencies, the refractivity N for air is given by the empirical relation[14,15]

$$N = (n - 1) \cdot 10^6 = \frac{77.6}{T}\left[p + \frac{4810e}{T}\right] \qquad [8.15]$$

where

p = barometric pressure, mbar (1 mm Hg = 1.3332 mbar)
e = partial pressure of water vapor, mbar
T = absolute temperature, K

Atmospheric refractivity depends on the pressure, temperature, and water vapor. Of these, water vapor is the most important at microwave frequencies. It strongly affects the speed of microwave propagation. Temperature variations are more significant than pressure variations. (It might be mentioned that although refractivity is generally not a function of frequency within the microwave region, atmospheric refraction at optical frequencies differs from that at microwave frequencies since it is more dependent on temperature than on water vapor.)

Since the barometric pressure p and the water-vapor content e decrease rapidly with height above the earth's surface, while the temperature decreases slowly, the refractivity normally decreases with increasing altitude. The decrease of N means that the velocity of propagation increases with altitude, causing the radar rays to bend downward. (Refraction of radar waves in the atmosphere is analogous to bending of light rays by an optical prism.) The result is an increase in the radar coverage, as was illustrated in Fig. 8.7a. The magnitude of the atmospheric refractivity at some particular altitude is not as important in determining the effect of refraction on propagation as is the small change of refractivity with height; that is, it is the *gradient* of refractivity that causes the rays to bend.

The major changes in atmospheric refractivity occur in the vertical dimension. There may be changes in the horizontal dimension as well; but these are generally small (especially over water) so that radar propagation can be considered independent of the azimuth direction, unless the radar ranges are very large. The path of radar waves in the atmosphere may be plotted using ray-tracing[16] techniques, provided the variation of refractivity with altitude is known.

Effective Earth's Radius A simple method to account for the effects of atmospheric refraction is to assume that the gradient of the index of refraction is constant with height, at least over the lower part of the atmosphere. This assumption allows the actual earth of radius a (a = 3440 nmi) and its nonuniform atmosphere to be replaced with an earth having a different radius (ka) and a uniform atmosphere in which radar waves propagate in straight

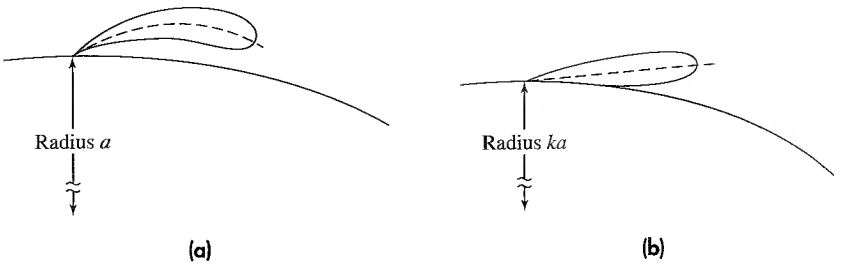

Figure 8.8 (a) Bending of the antenna beam due to refractian by the earth's atmosphere; (b) shape af the beam in the equivalent-earth representation with radius *ka*.

lines rather than along curved paths, Fig. 8.8. The factor k depends on the refractivity gradient at the surface. From Snell's law in spherical geometry, the value of k by which the earth's radius must be multiplied in order to plot the propagation paths as straight lines is

$$k = \frac{1}{1 + a(dn/dh)} \qquad [8.16]$$

where dn/dh is the rate of change of the refractive index with height. The vertical gradient of the refractive index is normally negative. The gradient of refractivity usually can vary from -79 to 0 N units per km of height.[12,13] The long-term average value of the gradient of N over the United States is approximately -39 N/km. When N is converted to n and substituted into the above equation, we get $k = 4/3$. The use of the $k = 4/3$ effective earth's radius to account for normal atmospheric refraction is convenient and widely used. It is only an approximation, however, and might not yield correct results when precise predictions are required. The term *standard refraction* is sometimes used to signify a value of $k = 4/3$ with the index of refraction decreasing uniformly with altitude with a gradient of $dn/dh = -39 \times 10^{-9}$/m.

The 4/3rd earth radius represents an average and should not be used where precision is important. The correct value of k depends on meteorological conditions and can be found by measurement. Bean[17,18] states that the average value of k measured at an altitude of 1 km varies from 1.25 to 1.45 over the continental United States during the month of February and from 1.25 to 1.90 during August. In general, higher values of k occur in the southern part of the country.

Distance to the Horizon The distance d to the horizon from a radar antenna at a height h may be shown from simple geometrical considerations to be

$$d = \sqrt{2kah} \qquad [8.17a]$$

where ka is the effective earth's radius and the height h above the surface is assumed to be small compared to the real earth's radius a. For a four-thirds earth, this relationship becomes

$$d \text{ (nautical miles)} = 1.23\sqrt{h(\text{ft})} \qquad [8.17b]$$

or,

$$d \text{ (km)} = 4.12\sqrt{h(\text{m})} \qquad [8.17c]$$

Equation (8.17) is often used as a measure of the line-of-sight coverage of a radar. This can lead to optimistic results since the propagation loss at the range d given by Eq. (8.17) can be quite high, as mentioned later in the discussion of diffraction in Sec. 8.6. The actual coverage of a radar can be less than given by the above simple geometric relation because of the large diffraction losses at the horizon. In spite of this, Eq. (8.17) has been widely used. It should be replaced, however, by diffraction calculations when it is important to know the maximum range at which a radar can detect low altitude targets.

Exponential Model of Refractivity A limitation in the use of the effective earth's radius model is that the gradient of refractive index dn/dh is not linear with altitude, but is better approximated by an exponential model, especially in the troposphere above an altitude of 1 km. The exponential decrease of refractivity with height has been given as

$$N = N_s \exp(-h/H_s) \qquad [8.18]$$

where

N_s = refractivity at the surface of the earth
h = height above sea level in km
H_s = scale height in km

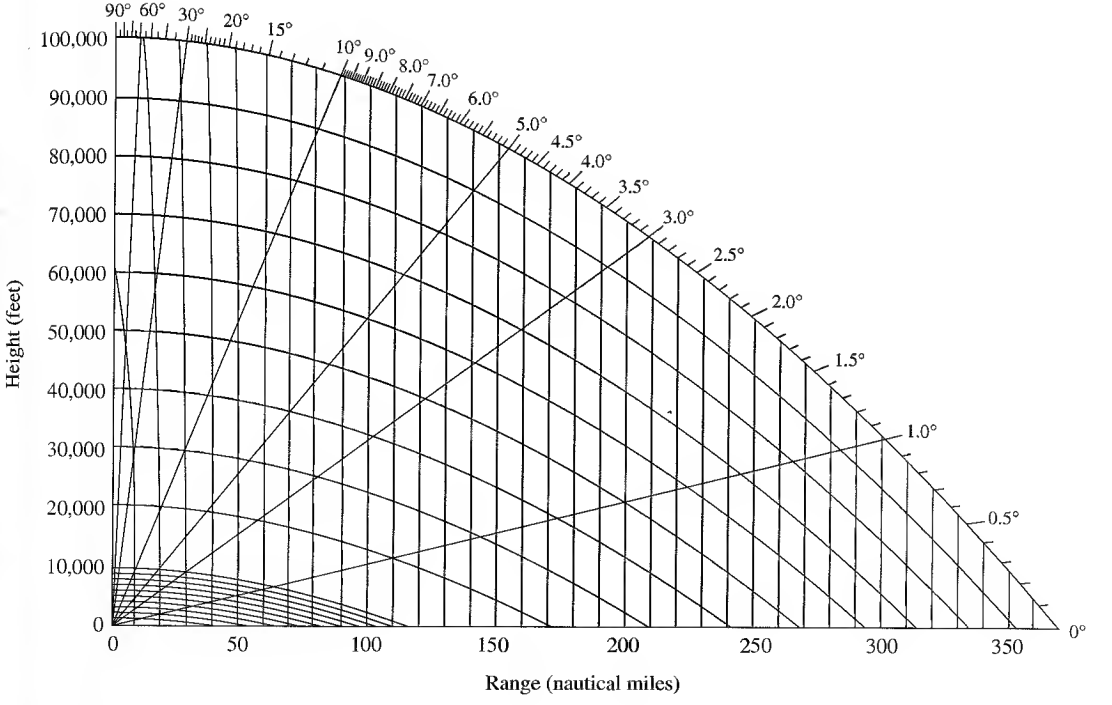

Figure 8.9 Radar range-angle-height diagram used to plot antenna coverage, based on the exponential model of refraction with $N_s = 313$.
(From Lamont Blake, *Radar Handbook*.[20])

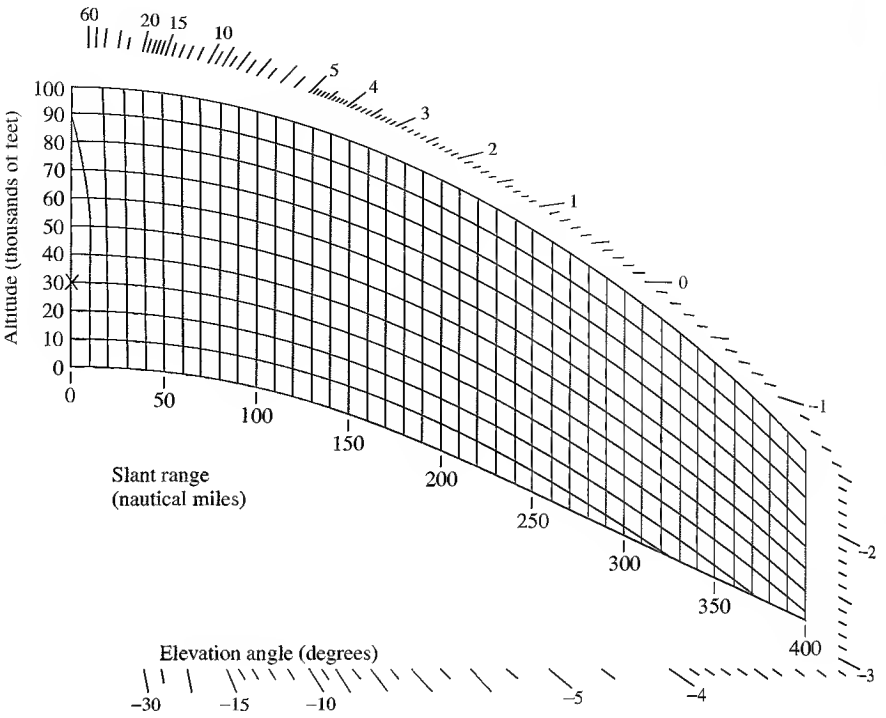

Figure 8.10 Radar range-height-angle diagram when the antenna is at an altitude af 30,000 ft and a U.S. Standard Atmasphere at 45° N latitutde in spring ar fall. Due ta W. G. Tank.[21]
(Reprinted with permission of Artech House, Inc., Norwood, MA. *www.artechhouse.com.*)

At mid-latitudes, the average value of N_s has been said to be 315 and the average value of H_s as 7.35 km.[19] Other values have been proposed, however.

An example of a range-height-angle chart (due to Lamont Blake) used to plot antenna coverage patterns based on the exponential refractivity model of Eq. (8.18) is shown in Fig. 8.9.[20] The surface refractivity is $N_s = 313$, and the scale height $H_s = 6.95$ km. In charts such as this, it is customary to plot height in feet and range in nautical miles.

Range-height-angle charts are often based on an antenna at ground level. When the radar antenna is elevated, as when on a tall mountain or when performing as an Airborne Early Warning (AEW) radar, these charts have to be modified. Figure 8.10 is an example due to W. G. Tank[21] for a radar at an altitude of 30,000 ft and a U.S. Standard Atmosphere. This can be thought of as a nomogram for determining the angle of arrival by first selecting the radar altitude (30 kft in this example), and then laying a straight edge from the radar location to the target point. The angle of arrival is read on the angle scales around the edges of the figure. A slightly different approach for plotting the range-height-angle charts when the antenna is not at ground level was suggested by Bauer,[22] based on the CRPL exponential atmosphere.

Standard Atmosphere A *U.S. Standard Atmosphere* is a hypothetical vertical distribution of atmospheric temperature, pressure, and density which by international agreement and for historical reasons, is roughly representative of year-round mid-latitude (45°N) conditions.[23,24] At microwave frequencies, a model of the moisture as a function of altitude

must be added, which results in a refractivity $N = 316 \exp(-Z/26.5)$, for $Z \leq 25$, where Z = altitude in thousands of feet.

Radar Measurement Errors Due to Refraction As was illustrated in Fig. 8.7b, refraction causes the radar rays to bend and results in an apparent target height that is different from the true height. An example of the angular error as a function of height and elevation angle as calculated by Shannon[25] is shown in Fig. 8.11. He assumed $N_s = 313$ and $H_s = 7$ km. At an altitude of 40 kft and an elevation angle of 3° the angle error is 2.67 mrad (17.45 mrad equals 1°).

When precision measurements are required, corrections should be made to the radar data to obtain accurate elevation angle, target height and range.[26] Surface observations often are sufficient for ascertaining the effects of refraction, but there can be cases when the variation of refractivity with height is not simple (as in the case of ducting discussed in the next section). In these cases, the variation of refractivity with height has to be measured and ray-tracing methods used to determine the measurement errors.

Even without ducting or other nonlinear refractivity profiles, errors can be significant. A comparison of heights obtained with the 4/3rd earth-radius model and the exponential model can be found in Brown[27] (and repeated in Murrow[28]). For example, at a range of 100 nmi with $N_s = 315$, the exponential model predicts a height 200 ft greater than the 4/3rd earth-radius model, when the elevation angle is 0.5°. It results in a 500 ft greater height compared to the 4/3rd earth model when the elevation angle is 2.0°. At the same range of 100 nmi and an elevation angle of 2.0°, the exponential model gives a

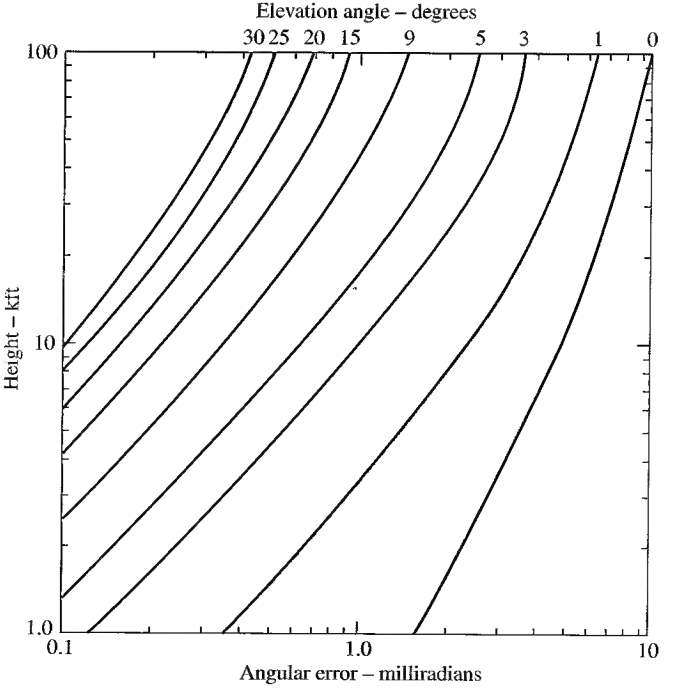

Figure 8.11 Calculated angle error (abscissa) due to atmospheric refraction for a standard atmosphere as a function of elevation angle and target height (ordinate.) (After Shannon.[25])

height error of 2.32 kft when $N_s = 370$ and an error of 1.38 kft when $N_s = 280$. The need for highly accurate knowledge of atmospheric refractivity limits the accuracy with which target height can be determined. This is the reason radar has not been used in the past when precision height measurements are needed.

In measurements to determine how well one can predict the effect of refraction, the accuracy of an AN/FPS-16 tracking radar was checked against photo theodolites at the U. S. Army Electronic Proving Ground, Fort Huachuca, Arizona.[29] The AN/FPS-16 is a highly precise tracker with rms mechanical and electronic measurement errors of ± 0.1 mrad for azimuth and elevation angles and ± 15 ft for range. At 40 nmi, the three-dimensional rms precision of this radar is ± 33 ft. Location measurements were made on aircraft at a range of 40 nmi and elevation angles from 0.7 to 2.8°. It was found that at an elevation angle of 2.5°, the rms elevation error was equal to the inherent ± 0.1 mrad precision of the radar. Above 2.5°, the predicted elevation errors were smaller than the inherent precision. Below 2.5°, the angle errors due to refraction were larger than the inherent radar precision.

There is also an additional time delay in propagating within the atmosphere that leads to an error in range. Shannon calculated this for the same conditions as for the angle error in Fig. 8.11. At 40 kft and an elevation angle of 3°, the range error is 97.5 ft. Shannon's plot can be found reproduced in Nathanson.[30]

A correction for the range error due to refraction, suggested by G. Robertshaw,[31] is given by the expression

$$R_c \cong 0.42 + 0.0577\, R_t \left(\frac{N_s}{h}\right)^{1/2} \qquad [8.19]$$

where

R_c = range correction, m
R_t = radar range, km
N_s = surface refractivity in N-units
h = radar altitude in kft

This expression was derived from ray-trace computations performed for radar altitudes of 15 kft, 35 kft, and 65 kft, based on a total of three months of measured atmospheric data over a period of three years at two sites in Germany, one in Saudi Arabia, and one in South Korea. It was said to have "the advantage of great simplicity with a tolerable loss of accuracy" and that "it will provide adequate range correction for airborne radar."

Measurement of Refractivity There are two basic methods for determining the refractivity profile of the atmosphere: one is the radiosonde, or equivalent, and the other is the refractometer.

Radiosonde The atmospheric refractivity profile may be obtained indirectly by the use of the empirical relationship given by Eq. (8.15) which equates refractivity with the properties of the atmosphere. The three measurements of water vapor pressure (humidity), atmospheric pressure, and temperature can be obtained with conventional

weather-observation instruments launched into the atmosphere on a balloon. Such an instrument is called a *radiosonde.* Radiosonde measurements are routinely obtained daily throughout the world. The accuracy of radiosonde weather measurements, however, is generally not as good as might be desired for radar propagation predictions. Furthermore, the temperature, pressure, and humidity are sampled sequentially rather than simultaneously, and the sampling interval for each measurement is approximately 100 m in altitude. This may be satisfactory for weather observations, but it can sometimes cause the radiosonde to miss the sharp changes in refractivity that are characteristic of the strong, but shallow atmospheric layers that give rise to nonstandard propagation conditions.

Helicopter Probes[32] In addition to having less than desired resolution in altitude, the conventional balloon-borne radiosonde makes one vertical pass and obtains only one vertical profile. The wind can cause it to move over a considerable horizontal distance during its flight and its measurements might not be representative of a true vertical profile. Furthermore, the measurements produced by conventional radiosondes launched from ships at sea might be contaminated by the microclimate created by the ship. A better method to probe the lower atmosphere where nonstandard propagation is prevalent is to mount instruments on a helicopter which can simultaneously provide the water vapor, pressure, and temperature as a function of range as well as altitude. A helicopter equipped by the Johns Hopkins University Applied Physics Laboratory (APL) employed more precise meteorological sensors than are normally found with weather radiosondes to obtain in almost real time the atmospheric refractivity. All three meteorological measurements were made at a data rate of 0.5 s. The altitude could be determined with a resolution of 0.3 m from 0 to 1000 m. These measurements were fed to a computer that calculated and displayed a continuously updated plot of modified refractivity versus altitude. The helicopter traveled with an airspeed greater than 30 m/s. Soundings were made with the helicopter ascending or descending at a rate of 1.5 to 3 m/s.

Small Rocket Probes[32] The meteorological measurements needed to determine refractivity profiles can be obtained with a simple, low-cost expendable rocket. It can be used when it is not practical or convenient to use a helicopter. Such a rocketsonde developed and employed by APL carried an instrument package weighing 453 g to an altitude of 150 to 800 m, where it deployed the instruments using a 1 m diameter parachute. Measurements can be made with a vertical resolution of 2 m, which are then telemetered back.

Refractometer An alternative to using meteorological measurements to indirectly derive the atmospheric refractivity is to use the more accurate and more responsive *microwave refractometer.* This instrument directly measures the index of refraction (or its square, the dielectric constant) by comparing the resonant frequencies of two identical microwave cavities. The resonant frequency of a cavity depends on its dimensions and its contents. One cavity is vented so as to sample the atmosphere; the other is hermetically sealed and acts as the reference. The cavities are fed by the same microwave source that is swept in frequency. The difference between the resonant frequencies of the sampled and reference cavities is a measure of the index of refraction. The microwave refractometer has much greater accuracy than the indirect measurement based on Eq. (8.15). It can

measure changes in refractivity of less than 0.1 N unit; and when used to determine variations about an undetermined mean, it can have a time constant that allows detection rates of up to 100 Hz.[33] Although the refractometer may provide excellent refractivity measurements, it might not be suitable for all applications since it requires an aircraft or helicopter. It is usually too costly to be expendable, as is a radiosonde or a rocketsonde.

8.5 NONSTANDARD PROPAGATION

The previous section described the effect on radar propagation of standard, or normal, refractive conditions. Refractive effects, however, can be much more complex than described by the standard exponential model, and can cause significant changes in radar propagation. Such conditions are known as *anomalous,* or *nonstandard, propagation.* As a rough generalization, when nonstandard propagation conditions occur, the maximum ranges of a surface radar for detecting low-altitude or surface targets might be extended from two to five times what would be expected with a uniform atmosphere.[34]

Normal refraction occurs when the refractive gradient with height, dN/dh, is between 0 and -79 N units per km of height. (Note that we have said previously that the long-term mean gradient over the continental United States is about -39 N/km.) When the gradient equals -157 N/km, the effective earth's radius as given by Eq. (8.16) becomes infinite. Rays that are initially horizontal will then follow the curvature of the earth. Under such conditions, the radar range is significantly increased and detection beyond the radar horizon can result. Refractive gradients between -79 and -157 N/km result in what is called *superrefraction.* When the gradients exceed -157 N/km, the curvature of the propagating ray exceeds the curvature of the earth and ducts can form that trap the radar energy. The trapped energy within the duct can propagate to ranges well beyond the normal horizon.

If the refractive gradient were to increase with height, instead of the more usual decrease, the propagating rays would curve upward and the radar range would decrease as compared to normal conditions. This is called *subrefraction.* Its occurrence is rare; but when it does occur, its effect can be serious. It has been suspected of causing ship accidents when using marine radar. The term nonstandard propagation, or anomalous propagation, applies to any of the above propagation conditions other than normal. Table 8.1 summarizes these refractive conditions.

There are three general classes of ducts that will be briefly described. These are evaporation ducts, which occur at the surface of the sea; surface-based ducts; and elevated ducts. The later two can occur over land as well as water. To propagate energy within the duct, the angle the ray makes with the duct should be small, usually less than about one-half degree. Therefore, only those rays launched nearly parallel to the duct are trapped.

Evaporation Ducts In a maritime environment, standard refractive conditions seldom appear, so that nonstandard conditions of some form are often present.[35] The most common type of anomalous propagation over the ocean and other large bodies of water is the evaporation duct. It is found at the surface, and is a relatively common occurrence. The air in

Table 8.1 Summary of Refractive Propagation Conditions

Refractive Condition	Gradient: N units per km
Subrefraction	Positive gradient
No refraction (uniform atmosphere)	0
Standard refraction (4/3rd earth radius)	−39
Normal refraction	0 to −79
Superrefraction	−79 to −157
Trapping, or ducting	−157 to $-\infty$

contact with the sea surface is usually saturated with water vapor so that its relative humidity is almost 100 percent. The air several meters above the sea surface is not usually saturated so there will be a decrease in humidity from the surface value to the ambient value determined by the general meteorological conditions well above the surface. The rapid decrease of water vapor causes a rapid decrease of refractivity that results in the formation of a low-lying duct that traps the radar energy so that it propagates close to the sea surface. Ducting can cause the radar ranges for targets at or near the sea surface to be considerably greater than the free-space range.

Duct Height The "height" used to characterize an evaporation duct is not the height below which an antenna must be located in order to obtain extended propagation. It is more a measure of the strength of the duct. Evaporation duct heights, which typically might have values from 6 to 30 m, vary with the geographic location, season, time of day, and wind speed. Of the factors that can affect the strength of a duct, the wind speed seems to be of special importance. In one set of experimental observations conducted in the Atlantic trade wind region off the east coast of Antigua with X- and S-band radars, it was said that the wind was the only meteorological factor that was correlated with the rate of attenuation in the duct.[36] Wind speeds from 8 to 15 kt produced a moderately strong duct of low height. Winds from 20 to 30 kt produced a greater duct height, but in this case the duct was weaker according to the meteorological predictions. The attenuation in the duct, however, decreased with increasing wind. Passing squalls and rain showers did not affect the duct or decrease the propagated signal strength. The duct heights varied from 20 to 50 ft and were found to exist all the time during these experiments.

Evaporation duct heights cannot be readily determined by standard radiosondes or refractometers. They can be inferred, however, from theoretical models based on meteorological measurements. One such model due to H. Jeske[37,38] and modified by Paulus[39] utilizes the sea-surface temperature, air temperature, relative humidity, and wind speed—the last three being obtained at some reference altitude (often taken to be 6 m).[38,40] Table 8.2 gives the calculated average duct height, for various areas of the world, based on this formulation using meteorological measurements from a 15-year subset of data from the National Climatic Data Center.[41] The histograms for evaporation-duct heights for three of

the areas in Table 8.2, plus the worldwide average are shown in Fig. 8.12. (These were originally given in Ref. 41 in 2-m increments of height, but here a smooth curve was drawn.)

The predicted evaporation-duct height using the Jeske-Paulus model does not always agree with actual observations of radar propagation. This might be due, in part, to the difficulty in making the relevant meteorological observations at sea with sufficient accuracy. Also, the theory and the accompanying simplifying assumptions on which the predictions are based might not be applicable under all conditions, especially when large duct heights are predicted. The nature of an evaporation duct can be more complex and varying than are accounted for in a simple model.

An improved method of determining the evaporation duct height has been proposed by Babin, Young, and Carton, which they call *Model A*.[42] They take advantage of the availability of high-speed desktop computers, not available when the Jeske-Paulus model was first formulated, to eliminate some of the assumptions that were originally made, incorporate more atmospheric boundary-layer physics, and decrease the use of empirical relationships. This model not only provides a more accurate duct height, but it also gives the standard deviation of duct heights based on the accuracy of the sensors used to obtain the atmospheric data.

Frequency Dependence The thicker the duct, the lower the frequency that can be propagated; but there is a limit. The lower frequency limit for propagation within an evaporation duct is said to be about 3 GHz.[13] An approximate model for propagation in an evaporation duct is that of a waveguide with the sea as the bottom wall and a leaky top wall. Thus there is a low-frequency cutoff for propagation in this type of leaky waveguide.

According to Hitney,[13] a rough guide to the lowest frequency that can be trapped by a duct of a given height is as follows: 3 GHz requires a duct height of at least 25 m; 7 GHz, 14 m; 10 GHz, 10 m; and 18 GHz, 6 m. As the frequency increases, however, the propagation loss increases due to attenuation caused by the high concentration of water

Table 8.2 Calculated average height of the evaporation duct[41]

Area	Average Duct Height, m
North Atlantic	5.3
Canadian Atlantic	5.8
East Atlantic	7.4
North Pacific	7.8
Mediterranean	11.8
West Atlantic	14.1
Persian Gulf	14.7
Indian Ocean	15.9
Tropics	15.9
World Average	13.1

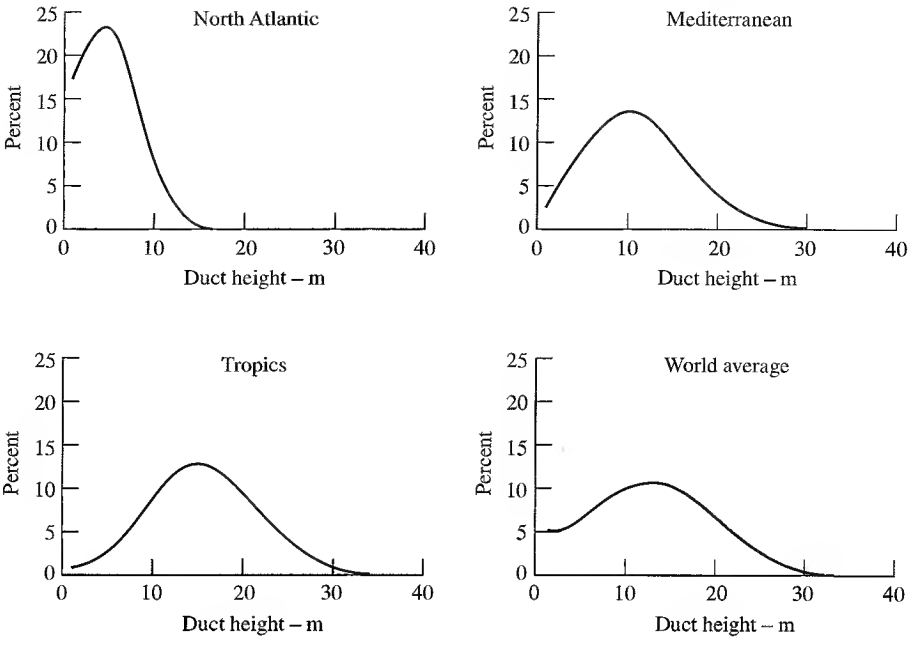

Figure 8.12 Examples of the statistics of evaporation-duct height for three areas of the world and the worldwide average, as given by Hitney et al.[41] These were calculated based on historical average meteorological measurements.

vapor within the duct as well as the attenuation due to a rough sea surface. For this reason Hitney suggests that the optimum frequency for duct propagation is around 18 GHz. Significant ducting has been observed, however, at frequencies as high as 94 GHz. Experiments at 94 GHz conducted over a 40.6 km over-the-horizon path along the Southern California coast found that the median loss with ducted propagation was 60 dB less than the loss that would have been obtained if there were no ducting (as with a standard atmosphere).[43]

Multiple-Mode Propagation If the duct height is large enough, more than one mode can be propagated. (A *mode* is a configuration of electric and magnetic field distribution, similar to the modes of propagation in a conventional waveguide.) Multiple propagation modes have two consequences: (1) the signal strength will not vary uniformly throughout the duct and (2) there can be more than one antenna height suitable for low-loss propagation. In normal propagation within a uniform or a standard atmosphere, the propagation loss decreases with increasing antenna height. The higher the antenna the better. On the other hand, with a single mode of propagation in an evaporation duct, the loss will increase with height within the duct. Propagation is better with a low-sited antenna. With a duct height that supports multiple modes of propagation, there can be more than one choice of antenna height that provides low-loss propagation. In one particular *X*-band experiment, the minimum attenuation occurred with an antenna height of 2 m.[36] Increasing the antenna height increased the loss until a maximum loss was found at about 10 m. Further increases of height decreased the attenuation again until a secondary minimum was

obtained at 20 m height, after which the attenuation increased (at least to a height of 30 m). On a ship, because of the pounding of the waves, it might not be practical to site a radar antenna 2 m over the sea if it were desired to obtain the benefits of ducted propagation. Instead, in this particular case, the antenna could be located at 20 m height, with a slightly greater loss being the price to be paid for the more convenient antenna location. These values apply to a particular location at a particular time. On most ships one probably would not want to have a variable antenna height to maximize propagation in the duct. What this example illustrates is that a fixed high-sited antenna might be a suitable compromise, rather than try to place an antenna in the duct at a low height where it can be subjected to destruction by the force of the waves.

Theoretical models of ducted propagation confirm the general nature of the above experimental observations.[44] Each mode of propagation of a guided wave has a particular configuration of electric field strength. When multiple modes are present, the fields of each mode can interfere constructively or destructively with the others. Consequently, the field strength along the duct or across the duct might not be uniform, which can lead to variations in the radar echo signal strength. When multiple modes of propagation are present in the duct, theory predicts considerable variation of the signal strength, called *fades*, because of the interference among the several modes. Fades can be of the order of 20 dB. In one example, it was shown that fading was strongly dependent on the height of the radar and the target, and for centimeter wavelengths the fading occurred at intervals of from two to three miles. Because of the strong dependence with height, the negative effect of holes in the coverage might be reduced by having more than one antenna, each at a different height, to provide height diversity. Frequency diversity might also reduce the effects of the holes in the coverage, if the frequencies are widely separated.

Ducting Within or Near the Horizon Most of the above has been concerned with propagation in a duct beyond the normal horizon. Within the horizon, the refractive effects of the duct can lead to a modification of the normal lobing pattern caused by the interference of the direct and surface-reflected rays discussed in Sec. 8.2.[45] The relative phase between the direct and surface-reflected rays can be different in the presence of the duct, and focusing[46] can change the relative amplitudes of the two components. Focusing by the atmosphere might even cause the amplitude of the surface-reflected ray to sometimes exceed that of the direct ray. The effect of the duct on line-of-sight propagation is to reduce the angle of the lowest lobe, bringing it closer to the horizon.

Although the evaporation duct provides a significant increase in signal strength for ranges well beyond the horizon, compared to what would be received if there were no ducting, it results in reduced signal strength at or near the horizon. This is illustrated in Fig. 8.13 which shows the propagation loss as a function of range for an X-band radar (where propagation loss is defined here as the ratio of transmitted to received power assuming that the antenna pattern is normalized to unity gain).[47] The presence of a duct increases the signal at the longer range compared to no duct, but it decreases the signal at the first lobe (about 10 dB for the 16 m duct) and it shifts the first null to longer range than when no duct is present. This confirms what was said in the previous paragraph about the evaporation duct lowering the lowest lobe.

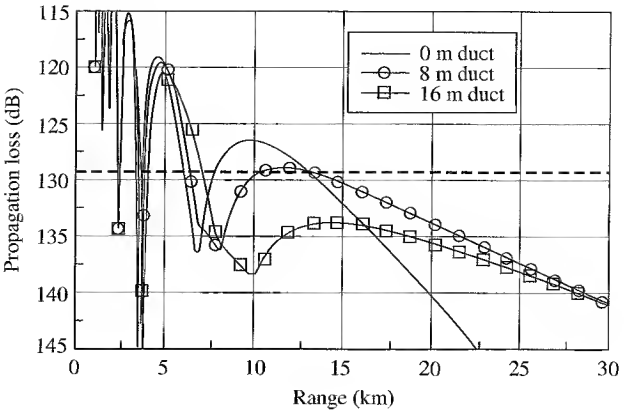

Figure 8.13 Propagation loss between radar and target as a function of range for an *X*-band radar located 23.5 m above the sea with a point target 4.9 m above the sea. The radar has a free-space range of 7.5 km. The dashed horizontal line represents the detection threshold for this radar. The "0 m duct" corresponds to a standard atmosphere. (From Anderson,[47] Copyright 1995 IEEE.)

Surface-Based Ducts[48,49] A surface-based duct is one whose base is at the earth's surface. There are three types of such ducts depending on the relationship of the trapping layer to the earth's surface. One example is the evaporation duct discussed in the above. The evaporation duct, however, is usually considered separately (as was done here) because of its unique characteristics and because it is a nearly permanent worldwide feature.[38] The second is a surface duct created from an elevated trapping layer, and the third is a surface duct created from a surface-based trapping layer. In this subsection, only the latter two will be considered, since the first has been discussed.

Surface-based ducts are formed when the upper air is exceptionally warm and dry compared with the air at the surface. There are several meteorological conditions that may lead to their formation. Over land, a surface-based duct can be caused by the radiation of heat from the earth on clear nights, especially in the summer when the ground is moist. The earth loses heat and its surface temperature falls, but there is little or no change in the temperature of the upper atmosphere.[50] This leads to a temperature inversion at the ground and a sharp decrease in moisture with height. Thus over land, ducting is most noticeable at night and usually disappears during the warmest part of the day.

Another cause of surface-based ducts is the movement (advection) of warm dry air, from land, over cooler bodies of water. Examples of such advections are the Santa Ana wind of Southern California, the sirocco of southern Mediterranean, and the shamal of the Persian Gulf.[38] Warm dry air that is blown out over the cooler sea is cooled at its lowest layers to produce a temperature inversion. At the same time, moisture from the sea is added to produce a moisture gradient, and a surface-based duct can be formed. This type of ducting tends to be on the leeward side of land masses, it occurs either during the day or night (but more likely to occur in the late afternoon or evening when the warm afternoon air drifts out over the sea), it might extend out over the ocean for several hundreds of kilometers, and it can last for long periods of time (several days).

The height of surface-based ducts generally does not exceed a few hundred meters. Propagation within a surface-based duct is relatively insensitive to frequency, and long-range propagation can occur at frequencies exceeding 100 MHz. Ducted propagation has

even been reported for frequencies down to 20 MHz.[51] Most of the reports of unusual long-range radar detection are due to this form of duct. A classic example is the often cited detection in the Indian Ocean during World War II by a 200 MHz radar located at Bombay, India. This radar, located 225 ft above sea level, frequently detected echoes from points in Arabia at ranges from 1000 to 1500 miles during the hot season. It was quite common to plot ships out to ranges of 200 miles, and cases were reported to 700 miles. By contrast, during the monsoon season when propagation conditions were more normal, the radar was able to plot ships out to a range of only about 20 miles.

An example of the effects of surface-based ducts is shown in Fig. 8.14. This is a plot of the two-way propagation factor (ordinate) seen in the vertical plane at a range of 50 nmi. The abscissa is the height above sea level. The radar frequency is 900 MHz and antenna height is 85 ft. The dashed curve represents the calculated propagation factor for a standard atmosphere. (According to Eq. (8.10) the peak of the lowest lobe due to multipath is predicted to be at 0.18°, and the peak of the second lobe is at 0.55°.) The solid curve was calculated for a nonstandard atmosphere whose refractivity profile was measured in the Persian Gulf at local noon on a day in August. The duct height was of the order of 700 to 800 ft. The signal strength below the duct height is considerably increased compared to the no-ducting standard-atmosphere situation. The increase in energy at the lower altitudes is accompanied by a decrease in energy in the lowest lobe below about 0.5°. The maximum of the two-way radar signal in the lowest lobe is seen to decrease by about 10 dB with ducting present.[52]

Surface-based ducts may also be formed by the diverging downdraft of air under a thunderstorm.[50] The relatively cool air which spreads out from the base of a thunderstorm results in a temperature inversion in the lowest few thousand feet. The moisture gradient is also appropriate for the formation of a duct. Although duct formation by a thunderstorm might not be as frequent as other ducting mechanisms, it may be used as a means of detecting the presence of a storm. An operator carefully observing a radar display can detect the storm by the sudden increase in the number and range of ground echoes. The conditions appropriate for the formation of a thunderstorm duct might have a duration of from one-half hour to a few hours.

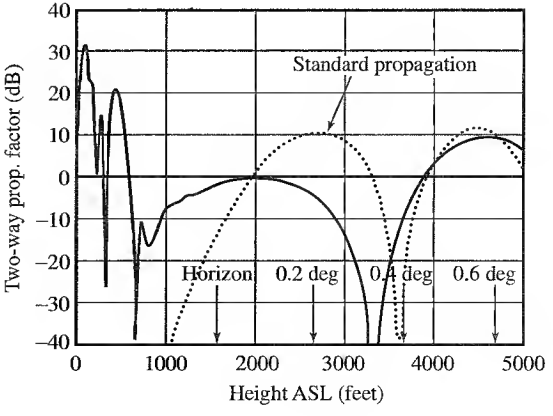

Figure 8.14 The solid curve is the two-way propagation factor as a function of height above sea level (ASL) for a surface-based duct taken in the Middle East at a range of 50 nmi measured at local noon on a day in August. The dashed curve represents the propagation factor calculated for a standard atmosphere.

(Courtesy of John Walters and Vilhelm Gregers-Hansen, NRL Radar Division.)

Elevated Ducts[38] The base of an elevated duct lies above the surface of the earth. Elevated ducts can occur in the tradewind regions between the mid-ocean high-pressure cells and the equator. Semipermanent high-pressure areas are centered at approximately 30° north and 30° south latitudes over the ocean. The region between these high-pressure areas and the equator are called the tradewinds. Two such tradewind areas that have been studied lie between Brazil and the Ascension Islands[53] and between Southern California and Hawaii.[54] Within the high-pressure regions, there is a slow-sinking of high-altitude air (called large-scale *subsidence*) which meets low-level maritime air (marine boundary layer) flowing toward the equator. The general sinking of air from high altitudes causes compression which results in adiabatic heating and a decrease in moisture content. This leads to warmer, drier air lying above cooler, moist air to produce a temperature inversion (an increase in temperature that causes a decrease in refractivity with height). The result is a strong duct along the interface of the temperature inversion along the top of the marine boundary layer.

In some cases, a stratus cloud layer will form at the base of the temperature inversion, and the duct altitude can be identified by the height of the cloud tops that are suppressed by the temperature inversion.[55] When the temperature inversion occurs below the altitude at which clouds are formed, a haze layer in the air below the temperature inversion can be observed.

The altitude of the tradewind duct varies from hundreds of meters at the eastern part of the tropical oceans to thousands of meters at the western end. Thus, the height rises gradually in going from east to west. Over the coast of Southern California, elevated ducts were found to occur an average of 40 percent of the time and have an average maximum elevation of about 600 m. On the western side of the Pacific Ocean along the coast of Japan, elevated ducts are said to occur 10 percent of the time and have an average maximum height of 1500 m.[38] The thickness of elevated ducts can range from near zero to several hundred meters. Frequencies as low as 100 MHz can propagate in the thicker elevated ducts. Since the elevated duct is due to meteorological effects, there can be seasonal as well as diurnal variations. It has been said, however, that elevated ducts give rise to strong persistent anomalous propagation throughout most of the year over at least one third of the oceans.

Ray-optics theory indicates that both the radar antenna and the target must be within the duct to obtain the benefits of the low propagation loss provided by the duct. In practice, it has been observed that this is not always necessary since enhanced propagation can occur with the radar and/or the target outside the duct (as defined by its classical duct thickness). This is likely due to the oversimplification of the duct model when defined by a smooth surface. Both the upper and lower boundaries of a duct can be irregular, allowing energy to "leak" or scatter into or out of the duct. It has been reported[56] that the presence of a very strong evaporation duct (height less than 100 ft) along with an elevated duct (at 2000 ft) can result in a significant increase in signal strength of a 3 GHz signal beyond the horizon at heights (3000 ft) which are an order of magnitude or more greater than the evaporation duct height.

The capability of elevated ducts to propagate to long range in the tradewind region is illustrated by a particular flight of an instrumented Naval Research Laboratory aircraft from San Diego, California, to Oahu, Hawaii. These were communications, rather than

radar, experiments. A 220-MHz signal was transmitted from an antenna located at an elevation of about 800 ft near San Diego. The transmitting antenna was within the duct. The signal was received by an aircraft throughout the entire path and was even detected after the aircraft was on the ground in Hawaii.[54] This long range, however, occurred only once during the fourteen runs conducted during these experiments. In all these runs, significant increases in range were achieved compared to what would be expected from tropospheric scatter propagation.

Meteorological conditions necessary for an elevated duct are similar to those for a surface-based duct. Under the proper conditions, one can turn into the other.[38]

Although enhanced propagation can occur when the target and the radar are properly located with respect to the duct, it is also possible to obtain reduced or no coverage above or below the duct, compared to that expected with a standard atmosphere. This lack of coverage due to the duct is called a *radar hole.*

Subrefraction The gradient of refractivity may, at times, be such as to bend electromagnetic rays upward rather than downward, causing a decrease in range when compared with standard refractive conditions.[57] This is called *subrefraction,* or *substandard propagation.* It occurs when the index of refraction increases with altitude, instead of decreasing as is the more usual situation. Subrefraction can occur when warm, moist air flows over a cool ocean surface or a over a cooler air mass just above the ocean surface.

An interesting example of subrefraction on radar performance has been reported by Brookner et al.[58] for an S-band marine radar located near the entrance to the Delaware Bay between the States of Delaware and New Jersey. The radar was operated by the Pilots Association of the Bay & River Delaware. Subrefraction was said to occur throughout the year in the Delaware Bay region. The radar typically had a range of 20 nmi for ships of interest, but when subrefraction occurred the range was reduced in half to 10 nmi. A one-way loss was observed that was greater than 20 dB relative to free-space propagation. Reduced conditions could last for several hours before returning to normal. Subrefraction results in an effective earth's radius less than one, and can be one half of the actual earth's radius. Some subrefraction conditions can produce a skip zone. For example, an approaching ship might be first detected at 20 nmi range, be undetected starting at about 12 nmi, and not seen again until it is within 6 to 8 nmi of the radar. It has been said that operating the radar antenna at a higher height above the surface can reduce the effects of subrefraction, but frequency diversity has little effect.

In some cases fog can lead to subrefraction. When fog forms, part of the water in the air changes from the gaseous to the liquid state, but the total amount of water remains unchanged. Water in liquid form contributes far less to the refractive index than water in the gaseous (vapor) form. The formation of fog near the surface results in a reduction of water vapor and a corresponding lowering of refractivity in the region of fog. The result is an upward bending of the radar rays, and a shortening of the radar range. Because other factors can enter, the presence of fog is neither a necessary nor a sufficient condition for the occurrence of substandard propagation.

It was mentioned in both references 57 and 58 that under some subrefraction conditions (and in the absence of fog), a ship that is not seen by radar might be seen visually.

This results because water vapor makes a significant contribution to the atmospheric index of refraction at microwave frequencies, but has little effect at optical frequencies.

Nonstandard Propagation over Land Much of the discussion about nonstandard propagation in this section has been based on overwater paths. Similar effects can occur over land; but there has been less written about overland effects than the effects that occur over water.

Over land, nonstandard propagation can be caused by radiation of heat from the earth on clear nights, especially in summer when the ground is moist. When the earth loses heat, its surface temperature falls, but there is little or no change in the temperature of the upper atmosphere. This leads to conditions favorable to superrefraction; that is, a temperature inversion at the ground and a sharp decrease of moisture with height. Thus over land masses, the phenomena of superrefraction and ducting are most noticeable at night and disappear during the warmest part of the day. Ducting observed over the Arizona desert during the winter when the atmosphere was clear and dry (low moisture content) has been attributed to this type of temperature inversion caused by nocturnal cooling of the ground.[59] In these experiments, the duct increased in height and intensity as the night progressed. It was also stated that "The cyclic variation in the meteorological conditions occurs with the same general character night after night and, in fact, year after year" and that "The field-strength variations reflect this consistency."

Terrain generally consists of high and low regions. Diffraction (forward scattering) from the high regions can have a significant effect on radar propagation and sometimes can be the dominant propagation mechanism.[13] In other cases, ducting may be dominant, but the profile of the terrain along the propagation path might reduce the strength of the duct.

The computation of radar propagation over irregular land surfaces is much more difficult than computations of propagation over the sea. The variation of refractivity with range must be taken into account when radar waves propagate over irregular terrain. The irregular features, including trees and other structures, are not easy to model realistically. The mathematical techniques must include diffraction as well as refraction effects. One approach has been to map the irregular terrain boundary into a rectangular domain where a numerical solution can be generated by applying well-established numerical methods.[60] The parabolic equation method, mentioned later in this section, is one of the computation techniques that have been applied to predict propagation over land since it can account for the variation of refractivity with range.

Effect of Ducting on Surface Clutter Measurements Most clutter measurements do not take account of the effects of nonstandard propagation. Ducting effects, when they exist, are usually inherent in the clutter data since it is difficult to separate them. Ducting can be, therefore, a major source of inaccuracy when trying to make quantitative measurements of the radar cross section per unit area (σ^0) of surface clutter.

Another reason why measurements of clutter are suspect when ducted propagation exists is that the precise grazing angle of the radar ray is not known. Even if the grazing angle were known, it is not easy to accurately determine the attenuation caused by ducted propagation (which is needed to determine the radar cross section of clutter).

Unfortunately, most of the available clutter data does not account for nonstandard propagation conditions. If the refractivity conditions of the atmosphere were accurately known (as with extensive measurements), it is possible in principle to extract the value of grazing angle* and the clutter cross section during ducted propagation.[61,62] This, however, is not easy to do in practice.

In the curves of sea clutter data shown in Fig. 7.13, the value of sigma zero (clutter cross section per unit area) for surface-based *X*-band radars did not drop off sharply at low gazing angles, as might usually be expected due to multipath from the surface. On the other hand, it was found that the *X*-band clutter echo did drop off with decreasing grazing angle, as expected when the radar was in an aircraft. It is suggested that this behavior might be due to the surface-based radars experiencing ducted propagation while the airborne radars flying above the evaporation duct did not.

It has also been observed in some cases with large radars looking at low angles over the ocean under ducted conditions, that echoes at long range from atmospheric clear-air turbulence can be much larger than the echoes from sea clutter.[63]

Occurrence of Ducting Ducting is essentially a fine-weather phenomenon (with the exception of thunderstorm ducts). Since tropical climates, other than at the equator, are noted for their fine weather, it is not surprising to find the most intense ducting occurring in such regions.[64] In temperate climates, ducting is more common in summer than in winter. It does not occur when the atmosphere is well mixed, a condition generally accompanying poor weather. When it is cold, stormy, rainy, or cloudy, the lower atmosphere is well stirred up and propagation is likely to be normal. Both rough terrain and high winds tend to increase atmospheric mixing, reducing the occurrence of ducting. Although windy weather which causes the atmosphere to be well mixed can inhibit the formation of ducts, experiments in the Atlantic trade wind region indicated that the wind was the most important meteorological factor required for the appearance of an evaporation duct.[36] Thus, evaporation ducts might be weak or even not exist if there were no wind at all.

Consequences of Ducted Propagation on Radar Performance Ducts can provide extended ranges against surface targets or low-flying aircraft considerably beyond the ranges that would be expected from a radar within a standard atmosphere. As previously mentioned, the radar antenna and the target must be in, or near to, the duct to experience extended range. Although ducts can significantly increase the range of a radar, the consequences of ducted propagation are not necessarily good. In fact, in most cases the negatives tend to outweigh the positives.

The ability to see at long ranges because of ducted propagation cannot be readily predicted in advance, and the increased ranges cannot be relied upon since they are not always present. One would certainly not want to depend on ducted propagation to extend the range of a radar when the proper ducting conditions for long range might not be available when needed. Furthermore, increased ranges in some directions are balanced by decreased ranges in other directions. There can be significant "radar holes" which prevent

*The grazing angle for sea clutter that can be found in this manner is the angle to the undisturbed sea surface. In practice, the angle the radar may make with the sea will depend on the slope of the large water waves on which ride the shorter waves as well as other surface disturbances.

a radar from seeing targets in some direction that would normally be detected if surface-based or elevated ducts were not present. The loss of detectability caused by radar holes can affect airborne radars as well as ground-based and shipborne radars. An aircraft or missile flying just above a duct might not be detected until it is at short range. A radar in an aircraft, such as for airborne air-surveillance, might not be able to detect targets that are below the duct even if they were well within the range of the radar. This can be avoided by proper control of the altitude of the aircraft carrying the radar, but it requires knowledge in real time of the local refractive conditions that can affect radar propagation.

Ducted propagation can make possible the detection of unwanted clutter echoes at long ranges that might otherwise not be detected in a normal atmosphere. This can place a severe burden on MTI radars designed on the assumption that clutter will not appear beyond a certain range. Also, multiple-time-around clutter echoes that arrive from beyond the maximum unambiguous range might not be eliminated if the doppler processing employs pulse-to-pulse staggered repetition periods.

In areas of the world where surfaced-based ducts can significantly extend the radar horizon for a large portion of the time, the greatly increased clutter echoes that are obtained can seriously degrade the performance of a radar not designed to cope with it. Such radars that experience the detrimental effects of ducting should be designed with a large dynamic range so as to avoid receiver saturation by large clutter echoes, the radar should have additional MTI or pulse doppler improvement factor to eliminate the larger than normal clutter, and the radar waveforms and processing should be designed to cancel multiple-time-around clutter echoes that originate from long ranges. The last mentioned is accomplished by using a constant prf (instead of pulse-to-pulse prfs) with processing that uses the required number of "fill pulses."[65] Fill pulses are those given zero weight in the digital MTI processor (that is, they are discarded) so as to eliminate pulse repetition intervals that do not have multiple-time-around clutter.

Again it should be mentioned that ducted propagation theoretically requires that the radar and target be within or close to the duct. It is seldom that a conventional surface-based radar, for example, will experience serious ducting effects if its beam is pointed to an elevation angle greater than about 0.5°.

Modified Refractivity In this section the refractivity, denoted by N, has been used to describe the property of the atmosphere to bend radar waves. It is sometimes convenient, however, to employ a modified refractivity, defined as

$$M = N + (h/a) \times 10^6 \qquad [8.20]$$

where h = height above the earth's surface, and a = earth's radius (in the same units as h). The modified refractivity M takes account of the curvature of the earth. It is useful in identifying ducting, since the trapping of radar waves occurs for all negative gradients of M. The modified refractivity, rather than N, is commonly employed by propagation engineers for determining the effects of refraction.

Prediction of Refractive Effects The theory of ducted propagation is not as complete as one might like. Available theoretical models sometimes fail to adequately describe what is taking place in nature. Nevertheless, there have been developed usable prediction

methods based on local meteorological measurements that provide estimates of how ducted propagation might affect the radar coverage and how the radar platform might be positioned to minimize the effects of nonstandard propagation. In the following are briefly described the several methods mentioned by Hitney[66] for determining the effects of refraction by a nonstandard atmosphere.

Ray Tracing This uses geometrical optics to determine the paths taken by radar waves as they propagate through the atmosphere.[67] In ray tracing the modified refractivity profile is assumed to vary only with height. The height is divided into small increments Δh, and Snell's law is applied with the small-angle approximation to determine the bending of a ray as it leaves a region of refractivity N at a height h and passes into a region of refractivity $N + \Delta N$ at height $h + \Delta h$. The refractivity at each increment of Δh is assumed to be linear. Since refractivity does not depend on frequency (within the normal range of radar frequencies), a single ray-tracing diagram can also be considered to be independent of frequency. Ray tracing is relatively simple compared to other models; but it does not provide the magnitude of the field strength. It also requires that the refractive index not change significantly in a distance comparable to a wavelength and the spacing between neighboring rays must be small in order to produce correct results when the rays diverge, converge, or cross. Also, diffraction effects are not taken into account.

Waveguide Model The trapping layer can be considered as a waveguide with multiple modes of propagation.[68] Those readers familiar with microwave propagation in metallic waveguides know that the dimensions of the waveguide usually are chosen so that only one dominant "mode" can propagate. In a rectangular guide this occurs when the broad dimension is slightly greater than a half-wavelength. If the dimensions are much larger than this, more than one mode of propagation can take place. Each mode has a different field configuration along the guide than the others. The various modes interfere or reinforce with one another as the energy travels along the guide, which is why a single mode of propagation usually is preferred. The theory and practice of propagation in waveguides was developed primarily in the 1930s and 1940s. The theory of guided wave propagation in other than metallic waveguides, however, is much older. It was first devised to explain how long-wavelength radio waves can propagate around the earth along the structure formed by the earth's surface and the ionosphere. Such a situation results in the energy propagating in more than one mode. A similar type of propagation occurs when sound waves travel in water when one surface of the guide is the bottom of the sea and the other is the sea surface. In a metallic waveguide, the walls present sharp boundaries that reflect the propagating waves incident upon them. Waves can also be reflected from a stratified medium in which the refractivity varies continuously and which has no sharp boundary. This is what happens in ducted propagation.

The theory of guided propagation in a layered medium has been applied to radar propagation in atmospheric ducts. This is a physical optics approach that takes into account propagation loss and diffraction. The theory predicts a cutoff frequency, below which no propagation can take place in the guide medium. The waveguide model can be employed when the vertical refractivity profile is independent of range (a vertically stratified, horizontally homogeneous atmosphere). Thus it is not suited when the atmospheric refraction

varies with range. It can be used for ducted propagation beyond the horizon. The mode theory applies best when only a few modes are present, and when both the radar and the target are well within the duct. It tends to predict greater loss than indicated by actual measurements when the radar, target, or both, are not within the duct. One reason for this is that the duct is usually *leaky*. The upper boundary of the atmospheric duct is not necessarily smooth, but can be ragged so that the simple model of a plane surface is not realistic. Another limitation is that mode theory when applied over land does not usually include the effects of scattering from the nonsmooth terrain which is characteristic of most of the earth's surface.

The effects of multiple modes on the propagation within a duct has been mentioned earlier in this section, in the subsection "Multiple-Mode Propagation." It was said there that fades due to multiple modes can be of the order of 20 dB and can occur at intervals of 2 to 3 mi in range.

Parabolic Equation Model Unlike ray tracing or the waveguide model, the parabolic equation method can handle refractive index changes that are inhomogeneous in both the horizontal and vertical directions. Thus it is useful whenever the refractivity profile varies with range; such as at land/ocean interfaces and in propagation over irregular terrain. This approach solves the Helmholtz wave equation with a parabolic equation approximation, such as a numerical method called the Fourier split-step algorithm.[69] The *split-step parabolic equation* provides an efficient method for modeling atmospheres where the vertical refractivity profile changes along the propagation path. It works well within the horizon and over the horizon as well as near the horizon, so that a single model can be used to make computations in all regions of interest. It has considerable advantage over prior methods, but it might require large computer resources of memory and run time. It has been noted[66] that rough surface effects are difficult to handle rigorously with this model. In addition to being applied over the ocean, the parabolic equation method has been applied to propagation over terrain.[70–72]

Hybrid Method The purpose of a hybrid method is to provide the benefits of the split-step parabolic equation (PE) method without the extensive computations. One example is the Radio Physical Optics (RPO) model that uses a combination of ray optics and split-step PE methods.[73] These two are complementary in that split-step PE works well for small angles and the ray optics works well at the higher angles not covered by the PE method. Hitney states that this hybrid method can be 100 times faster than the pure split-step PE method for stressful cases.

Computer-Based Propagation Assessment Methods There exist several computer software programs for determining the effects of propagation based on knowledge of the environmental factors that influence atmospheric refractivity. These have been used mainly by the military to determine the actual coverage of their radars under nonstandard propagation conditions. Much of the pioneering work in this area was performed by the SPAWAR Systems Center, San Diego (formerly called NRaD).

Figure 8.15 illustrates in a simple manner one example why the military tactical planner would be interested in knowing the radar propagation conditions to be expected.[74] The

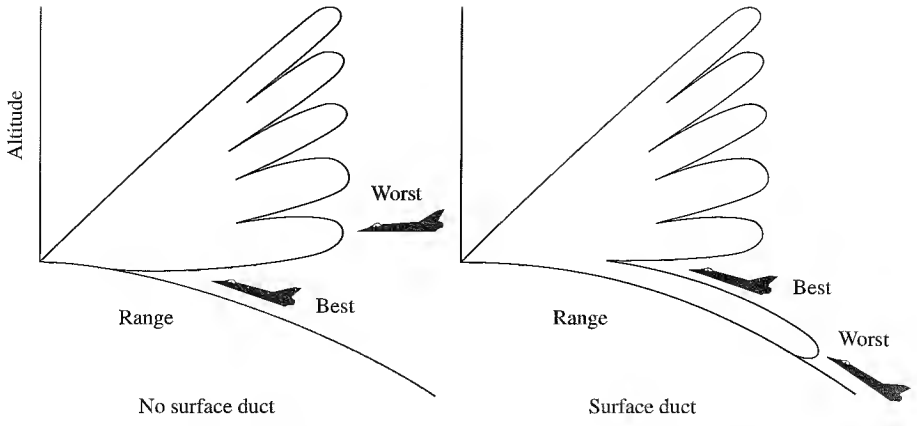

Figure 8.15 Sketch illustrating the effect of atmospheric ducting on the flight altitude of an attacking aircraft.
(From J. H. Richter.[74])

left-hand side of the figure shows the radar coverage that might be obtained under standard propagation conditions with no surface duct present. An attack aircraft could avoid detection at long range by flying at low altitude. If, on the other hand, a surface duct were present, as depicted on the right-hand side of the figure, a low-flying attacker would be detected at much longer range because of the ducted propagation. A better tactic under such circumstances would be to fly at an altitude just above the duct.

IREPS One of the first computer-based propagation prediction programs for operational use was *IREPS,* which stands for *Integrated Refraction Effects Prediction System.* It was developed by the SPAWAR Systems Center as an operational assessment tool for the U.S. Navy and was installed on major ships of the Fleet.[75,76] It was used with a PC, and had an interactive display. IREPS provided the following products:

1. *Propagation conditions summary.* The plot of refractivity as a function of height was shown graphically for the location, date, and time of day, along with a plain-language narrative assessment of what effects might be expected over surface-to-surface, surface-to-air, and air-to-air paths. The presence and vertical extent of any ducts were indicated, and wind speed and evaporation duct height were listed numerically. A correction for the measurement error of the target elevation angle due to bending by refraction was also given.
2. *Display of radar coverage.* These were vertical coverage diagrams (range versus height) for specific radars and other electromagnetic systems.
3. *Display of one-way path loss with range.*
4. *AEW aircraft stationing aid.* This showed the distortion of normal propagation caused by refractive effects at a given range for various combinations of radar and target altitudes. It provided the optimum location for the radar, so as not to lose targets

because of radar holes and allowed the aircraft to minimize detection by a hostile intercept receiver.

5. *Surface-search radar-range table.* This provided predictions of the detection range for an operator-selected surface-search radar against an operator-selected table of surface targets.
6. *Electronic support measures (ESM) intercept-range table.* A display was given of the maximum intercept range for an operator-selected ESM system (intercept receiver) against various operator-selected radars or other emitters.

In addition, IREPS could display the 50 percent probability of detection range of various size targets for an operator-selected forward-looking infrared (FLIR) system operating at various altitudes.

There were several methods by which IREPS obtained information about refractive conditions, depending on what was available. Refractivity could be obtained from radiosonde measurements (balloon borne instruments to determine upper atmosphere pressure, temperature, and water vapor pressure); aircraft-borne microwave refractometers; or inputs from surface meteorological measurements made on board the ship on which IREPS was located. When none of these were available, IREPS utilized a stored library of historic refractivity and climatology statistics as a function of the latitude, longitude, season, and time of day. When historic data was used, the output was a prediction of propagation performance in probabilistic terms. Also stored were the necessary system parameters for the various radars, communications, electronic warfare, and other electromagnetic systems whose predicted propagation performance was required. IREPS could make propagation predictions for frequencies from 100 MHz to 20 GHz.

Hitney[66] indicated that one of the most important uses of IREPS was for selecting the best flight profile for an attack aircraft attempting to penetrate the coverage of a hostile radar. Under normal (nonducting) propagation conditions, an attack aircraft flies most of the distance to its target at low altitude in order to be below the coverage of the hostile radar. If, on the other hand, a surface-based duct was predicted by IREPS, the defending radar detection range against low-altitude targets might be greater than when ducting was absent. Under such circumstances, it is usually better for the attacker to fly at an altitude slightly above the duct. Hitney has said that "the use of IREPS coverage diagrams in strike [attack] warfare flight profile selection has been verified operationally to be effective 85% of the time."

TESS, or Tactical Electronic Support System[66] This is designed for naval tactical decision making and is similar to IREPS in that it uses the same basic propagation assessment models and displays, but with better environmental information and some improved propagation models. For example, it employs the hybrid RPO model mentioned previously so as to take account of range-dependent refractive effects. It uses real-time satellite data, and has the ability to overlay this data with other meteorology analyses and forecasts. TESS is designed for surface ships that have officers trained in the environmental sciences, including aircraft and helicopter carriers and amphibious assault ships.

EREPS, or Engineer's Refractive Effects Prediction System[38] This is also derived from IREPS, but is designed for the use of engineers instead of naval tactical decision makers.

For example, the engineer is more interested in the long-term performance of a radar, usually in statistical terms, rather than in single-event performance prediction that IREPS was designed to provide as a tactical decision aid. EREPS is more flexible than IREPS in that it increases the user's ability to edit the various parameters and determine how changes in radar parameters affect performance. It also allows the use of a high-fidelity range-dependent propagation model such as the RPO program, including the use of the binary files of propagation loss versus range as generated by the RPO program.

AREPS or Advanced Refractive Effects Prediction Program (AREPS) This software program is an advanced version of IREPS that computes and displays radar probability of detection, electronic support measures (ESM) vulnerability, UHF/VHF communications capability, and simultaneous radar detection and ESM (intercept) vulnerability.[77] It is Windows based and is available from the SPAWAR Systems Center as a CD or from the Internet.

Other versions of computer-based propagation prediction methods have been reported by Ferranti Computer Systems, Ltd. of the United Kingdom[78] and by the Ukraine.[79] The original Ferranti system was called IMP, or Identification of Microwave Propagation. As described, it appears to have less capability than IREPS. The Ukrainian system is said to incorporate scattering from atmospheric turbulence.

8.6 DIFFRACTION

In the previous section we discussed how radar waves can propagate beyond the geometrical horizon of the earth by means of atmospheric refraction. Another mechanism that permits electromagnetic waves to extend beyond the geometrical horizon is *diffraction.* Radio waves are diffracted around the curved earth in a manner similar to the way light is diffracted by a straight edge (a topic usually covered in college physics courses). The ability of electromagnetic waves to propagate beyond the horizon by diffraction depends upon the frequency (the lower the better). At microwave radar frequencies there is very little energy diffracted by the earth's surface so that microwave radar coverage cannot be significantly extended beyond the line of sight by this propagation mechanism. Diffraction is important, however, for understanding HF surface-wave radar and for predicting the signal strength at or near the radar horizon at any radar frequency.

Frequency Dependence of Diffraction Figure 8.16 is a theoretical plot of the electric field strength (relative to free space) incident on a target as a function of the distance from the radar transmitting antenna. Both the transmitting antenna and the target are at a height of 100 m, and there is no refraction to extend the horizon. The geometrical horizon at 71.4 km is also the horizon distance for optical frequencies ($\lambda \rightarrow 0$). It represents the approximate boundary between propagation and no propagation for optics and infrared. As the frequency decreases (wavelength increases), energy propagates farther into the region beyond the geometrical horizon. As the wavelength increases, however, it is noted that there is a reduction of energy at the geometrical horizon as well as just within the

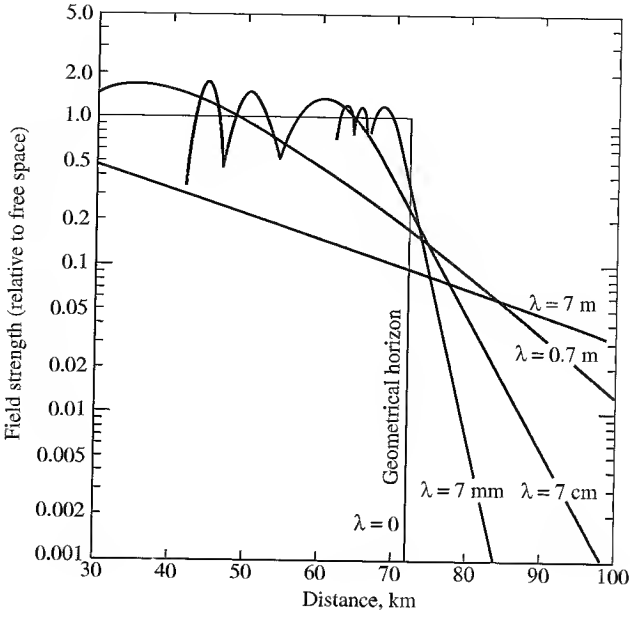

Figure 8.16 Thearetical field strength (relative ta free-space field strength) as a function of the distance fram the transmitting antenna. Vertical polarization, $h_a = h_t = 100$ m, $k = 1$, graund canductivity $= 10^{-2}$ mha/m, dielectric canstant = 4. (After Burrows and Attwood,[8] courtesy Academic Press, Inc.)

horizon. In the absence of refraction effects, microwave radar seldom has the ability to detect low-altitude targets beyond the geometrical horizon, or even at the horizon, unless it has sufficient power to overcome the loss caused by diffraction.

If low-altitude radar coverage is desired beyond the geometrical horizon in the diffraction region, the frequency should be as low as possible and there should be excess power to compensate for the diffraction loss. As an example, the loss in signal strength in the diffraction region at a frequency of 500 MHz is roughly 1 dB/mi at low altitudes. (It is even greater at higher frequencies.) Therefore, to penetrate 10 mi beyond the horizon within the diffraction region, the radar power at 500 MHz must be increased by 20 dB over that required for free-space propagation. Even if lower frequencies were available for radar to take advantage of the lower diffraction loss, the range resolution is poorer (because of narrower bandwidths), beamwidths are wider, the spectrum is crowded, and external noise increases with decreasing frequency.

If, on the other hand, the low-altitude coverage is to be optimized within the horizon in the interference region, Fig. 8.16 shows that the radar frequency should be as high as practical (consistent with other constraints on the choice of radar frequency).

Coverage at the Horizon The maximum "line-of-sight" distance d between a radar at a height h_a and a target at height h_t is given by the expression

$$d = \sqrt{2kah_a} + \sqrt{2kah_t} \qquad [8.21]$$

where k is the effective earth radius, and a is the earth actual radius. In this equation, the line of sight between the radar and the target is assumed to be tangent to the earth's surface. This equation is often used to describe the maximum range at which a target at an

altitude h_t can be seen above the radar horizon. The diffraction loss at the horizon, however, might be from 10 to 30 dB below that if in free space.[80] Thus caution should be used when employing the above equation to describe the low-altitude coverage of a radar when propagation is near the horizon.

Surface-Wave HF Radar The diffraction loss at HF frequencies (3 to 30 MHz) is much lower than that at microwave frequencies. For this reason, the potential of extended coverage at low altitudes beyond the horizon has been examined many times in the past using HF radar and the surface wave, or ground wave, mode of propagation where the diffraction loss is low. It has been said[81] that for every nautical mile increase in radar range beyond 75 nmi over the sea in the diffraction region requires an increase of radar energy of approximately 0.3, 0.5, and 0.6 dB per nautical mile at frequencies of 5, 10, and 15 MHz, respectively. The loss depends on the surface conductivity. Over land the loss is much higher than over the sea; which is why HF surface-wave radars are seldom considered for operation over land.

The lower the frequency the lower will be the propagation loss. The lower the frequency, however, the greater will be the external noise. (External noise can be many orders of magnitude greater than receiver noise). External noise is due to either atmospheric, cosmic, or anthropogenic noise. The radar cross section of most aircraft at HF is usually much larger than at microwave frequencies; but at a sufficiently low frequency (depending on the size of the target), the cross section falls in the Rayleigh region where it varies as the fourth power of the radar frequency. It then decreases rapidly with decreasing frequency. For example, the decrease in cross section of a fighter aircraft signifying the Rayleigh region might begin somewhere around 15 to 20 MHz. For a large bomber aircraft, the Rayleigh region might begin at a frequency of 3 to 6 MHz.

There will be an optimum frequency for a surface-wave radar. Below the optimum frequency there is an increase in radar power because of increased external noise and lower radar cross section. Above this frequency, increased power is also needed because of the increase in diffraction loss with increasing frequency. The optimum frequency will depend on the type of target and the variability of external noise with time of day and season. Because of the variability of external noise and the need to detect small as well as large targets, the choice of HF radar frequency is often a compromise. In one analysis of the optimum frequency for a particular HF radar, the region from 5 to 10 MHz seemed to be the best place to operate.[81]

Vertical polarization is used in HF surface-wave radar since its energy extends down to the surface, which is what is desired to detect targets at or near the surface. The energy radiated by a horizontally polarized antenna, on the other hand, decreases as the surface is approached. When surface-wave radars are considered for shore-based operation looking out over the sea, the antennas can be of large extent in the horizontal dimension. They might be from 300 to 1000 m (more or less). A 500-m antenna at 10 MHz has a beamwidth of about 4°. The antenna is an array which is either electronically steered in azimuth angle or which forms a number of multiple fixed receiving beams covering the area of interest. With multiple receiving antenna beams, the transmitting antenna is much smaller in size than the receiving array antenna since it utilizes one broad beam to cover the region viewed by the multiple, narrow receiving beams. The advantage of this antenna

arrangement is that it is easier to make a large receiving antenna than a large transmitting antenna. The multiple beams of the receiving antenna allow the simultaneous processing of the radar echo signals from each beam, which allows a faster data rate. Because of expense, HF radar antennas seldom have significant directivity in the elevation plane other than that obtained from a monopole radiator in front of a backscreen. These radars need doppler processing in order to detect desired moving targets in the midst of the large echo from the land or sea.

Because of the exponential diffraction loss, land-based HF surface-wave radars that look over the sea might have average powers of from several tens of kW to well over 100 kW. The pulse repetition frequencies are usually low so that ground echoes received via skywave propagation from long range do not interfere with target echoes from the near-range. The ranges of such radars might be from 50 to 150 nmi depending on the type of target. (Most of the numbers presented here are not meant to be interpreted as rigid bounds.)

HF surface-wave radars for shipboard operation have to be much smaller in size than land-based systems and be satisfied with lower power transmitters.[82] Their ranges would be correspondingly reduced. The main naval application for such radars might be to detect low-altitude antiship missiles at greater ranges than can be detected by microwave radar.

In spite of some attractive attributes of HF surface-wave radar there are many difficulties in their application (which mainly have been for military purposes). They have poor resolution in range and angle, no indication of target elevation angle (or height), they require large antennas, and on board ship, they can cause mutual interference with HF communications. If the chief interest is in detecting targets at over-the-horizon ranges, the radar cannot immediately differentiate between a target that is at the same range as the over-the-horizon target but at a higher altitude and within line of sight. Military radars for air defense require some form of target identification, usually a cooperative IFF (identification friend or foe) system that operates at microwave frequencies. Thus there is no convenient means for target recognition when using HF radar. Also, the powerful HF signals radiated by a military radar can be detected by a hostile intercept receiver at very long distances. Thus there are reasons why the HF surface-wave radar has not seen operational application even though it has the capability of seeing over the horizon.

In general, the long-range HF over-the-horizon radar that employs skywave propagation has greater range and greater coverage than a surface-wave radar, and is not that much larger than the largest surface-wave systems.[83] Much smaller HF surface-wave radars have also been operated at within-the-horizon ranges for remote sensing of sea state,[84] surface currents,[85,86] and icebergs.[87,88]

8.7 ATTENUATION BY ATMOSPHERIC GASES

Water vapor and oxygen in the clear atmosphere can attenuate radar energy when the radar frequency is at or in the vicinity of one of the resonant frequencies of these molecules. Figure 8.17 shows the attenuation due to both water vapor and oxygen as a function of frequency. There is a resonance peak of water vapor at a frequency of 22.2 GHz, and another in the millimeter wave region at 184 GHz.[89,90] The attenuation due to water

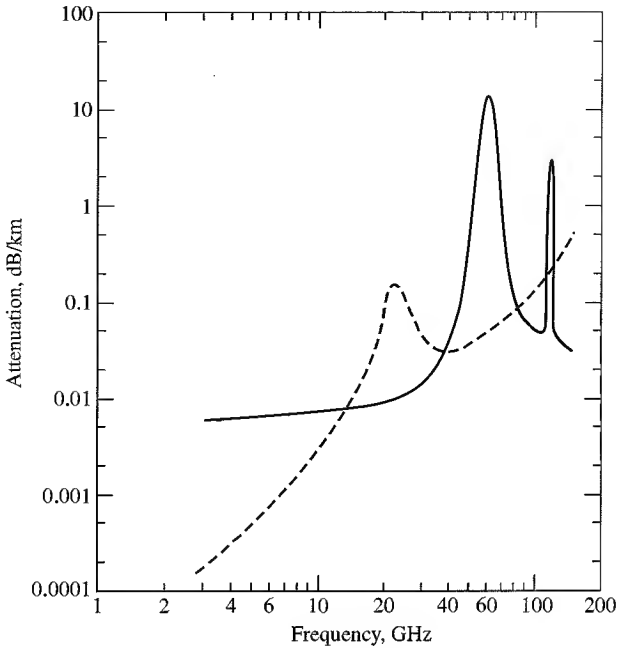

Figure 8.17 Attenuotion of electromognetic energy by otmospheric goses in an atmosphere at 76 cm pressure. Doshed curve is obsorption due to woter vopor in on otmosphere contoining 1 percent water vapor molecules (7.5 g woter/m^3). The solid curve is the obsorption due to oxygen. (Fram Burraws and Attwoad[8] and Straitan and Tolbert.[89])

vapor will depend on the amount of moisture in the atmosphere, which can vary with time and place. Although the attenuation is only about 0.2 dB/km at a frequency of 22 GHz, absorption can be sufficient to deteriorate the effectiveness of radars that operate at the original K-band frequency of 24 GHz. When radars were first developed at K band during World War II, it was not realized that there was a nearby absorption band. To avoid this problem, the original K band was split into a lower band, K_u, and an upper band, K_a. Table 1.1. Radars are almost never found any more at the original K band. The oxygen molecule has resonances at 60 GHz and 118 GHz. The 16 dB/km attenuation at 60 GHz makes this region unusable except for very short range radars and radars that operate in space outside the atmosphere.

Atmospheric attenuation generally has negligible effect on radar performance at the normal microwave frequencies. It begins to be increasingly important at frequencies above 10 GHz. The large attenuations experienced at millimeter wavelengths is one of the chief reasons why long-range radars are seldom found above 40 GHz.

The effect of attenuation, when it is large enough to be a problem, is accounted for in the radar range equation by inserting into the numerator the multiplicative factor $\exp[-2\alpha R]$, where α is the one-way attenuation coefficient measured in units of distance^{-1}, and R is the range to the target. Instead of α it is more usual to express the one-way attenuation, especially when plotted in graphs, as decibels per unit distance—which is what is done here. This is equivalent to the quantity 4.34α, where the constant 4.34 accounts for the conversion from the natural logarithm to the base 10 logarithm.

If the attenuation per unit distance α is not constant, $\exp[-2\alpha R]$ should be replaced by $\exp[-2\int\alpha(R)dR]$, with the integration taken from 0 to the target range R.

Atmospheric attenuation decreases with increasing altitude (there are fewer molecules to absorb the radar energy). When the antenna beam is pointed at some elevation angle, the variability of attenuation with altitude must be taken into account when determining the total attenuation along the propagation path. With a ground-based radar the attenuation is greatest when the antenna points along the horizon, and is least when it points to the zenith. For example, at the water vapor absorption line located at 22.2 GHz, when the energy is directed at the horizon (elevation angle of 0°), the total attenuation in propagating completely through the earth's troposphere and back again is 80 dB, a formidable number. When the energy propagates at the zenith (elevation angle of 90°), the total two-way attenuation through the entire troposphere is only 1.3°. If the elevation angle were greater than 10°, the total attenuation is less than 7 dB, so that when the radar is looking at the higher elevation angles, attenuation might not be important. Figure 8.18 gives

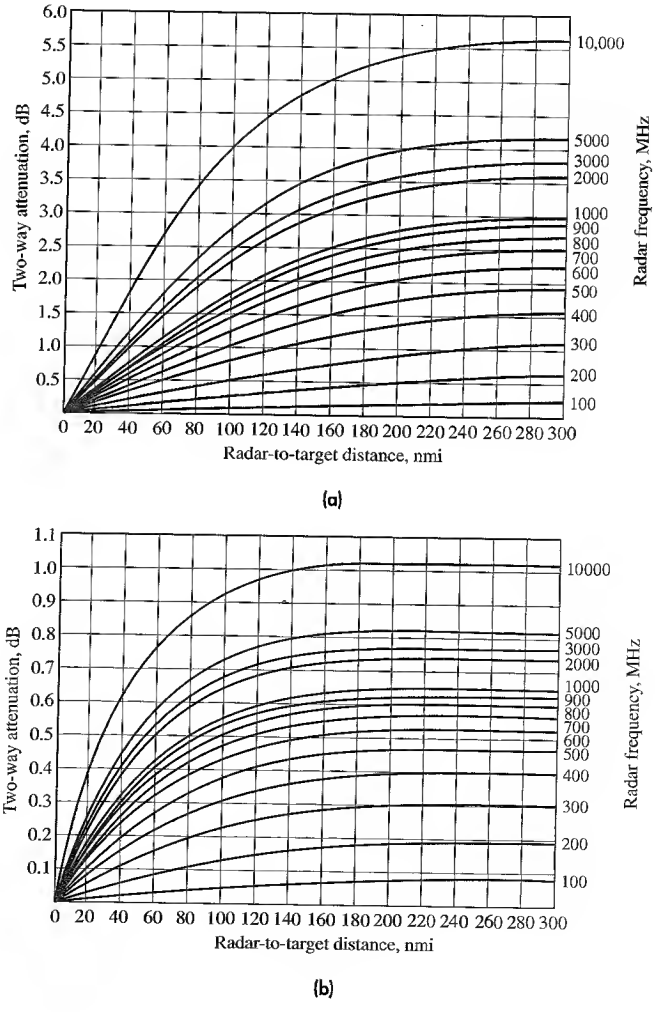

Figure 8.18 Two-way atmospheric attenuation as a functian af range and frequency far (a) 0° elevatian angle and (b) 5° elevation angle. (Fram L. V. Blake.[91])

examples of the two-way attenuation in the atmosphere as a function of range and frequency for elevation angles of 0 and 5°.[91] It might be noted that even if there were no loss at 0° elevation, the null at the horizon due to multipath prevents significant propagation of radar energy at or near this angle (except under ducting conditions or at low frequencies with vertical polarization.)

8.8 ENVIRONMENTAL, OR EXTERNAL, NOISE

The inherent internal noise of the radar receiver is what usually limits the detectability of targets by microwave radars (in the absence of clutter echoes). At frequencies at either end of the microwave spectrum, however, the limitation on sensitivity is usually the external noise that appears at the antenna terminals from some outside source. The reradiation noise due to atmospheric absorption usually determines the receiver sensitivity at the upper end of the microwave spectrum and at millimeter waves. At VHF and lower frequencies the receiver sensitivity is usually set by cosmic noise, the noise due to the combined effects of lightning strokes throughout the world, and anthropogenic noise. The minimum noise occurs at the middle of the microwave region, in the vicinity of S band. Generally, external noise is not a factor in radar performance unless the radar frequencies are outside the range of the usual microwave frequencies. Harmful external noise at the antenna terminals due to deliberate hostile jamming, however, can cause serious degradation to an unprepared military radar system, but this is not the subject of this chapter.

Atmospheric Absorption Noise It is known from the theory of blackbody radiation that any body that absorbs energy reradiates the same amount of energy that it absorbs, else it would increase in temperature. As mentioned in Sec. 8.7, water vapor and oxygen absorb (attenuate) radar energy. This absorbed energy must then reradiate as thermal noise. If L is the loss of radar energy when propagating through the atmosphere, and T_a is the ambient temperature of the absorbing atmosphere, the effective noise temperature of the reradiated energy is $T_e = T_a(L - 1)$. (The effective temperature is defined in Sec. 11.2.) Atmospheric absorption noise, just like atmospheric attenuation, is of potential concern only at the higher radar frequencies. Figure 8.19, shown later, is a composite plot of the several sources of electromagnetic noise as a function of frequency. Atmospheric absorption noise is the dominant effect at the right side of the figure. The maximum value of atmospheric absorption noise occurs for an elevation angle of 0°, the minimum values for an elevation angle of 90° (looking straight up).

Cosmic Noise There is a continuous background of noiselike electromagnetic radiation from extraterrestrial sources in our own galaxy (the Milky Way), extragalatic sources, and radio stars. Cosmic noise generally decreases with increasing frequency and can usually be ignored at frequencies above UHF. The magnitude of cosmic noise depends upon the portion of the celestial sphere to which the antenna points. It is a maximum when looking toward the center of the Milky Way, and a minimum when observing along the pole about which the Milky Way revolves. The maximum and minimum *brightness temperature* due to cosmic noise is shown in the left-hand portion of Fig. 8.19. The brightness

temperature can affect the system noise temperature and the sensitivity of the radar receiver (especially at the lower frequencies). In the absence of any radio stars, the background cosmic noise left over from the "big bang" at the start of the universe is the minimum noise level that might be expected. Its value is 2.7 K, which is too small to bother any radar receiver.

The sun is a relatively strong emitter of noise if the radar antenna beam directly views the solar disk. It might also be detectable with radars having poor sidelobes and very sensitive receivers. The minimum level of solar noise is due to blackbody radiation at a temperature of 6000 K. Solar storms (sunspots and flares), however, can increase the solar-noise level several orders of magnitude over that of the quiet or undisturbed sun. Radar stars are too weak to be a serious source of interference. Both radio stars (in conjunction with sensitive receivers) and the sun have been used as sources to calibrate the beam-pointing (boresight) of large antennas.[92–94]

Atmospheric Noise (Lightning) A single lightning stroke radiates considerable RF noise power, especially at the lower frequencies. At any one moment there are an average of 1800 thunderstorms in progress in different parts of the world. From these storms about 100 lightning strokes take place every second somewhere in the world.[95] The combined effect of all the lightning strokes is to give rise to a noise spectrum that is especially large at broadcast and shortwave frequencies. Noise radiated by lightning strokes throughout the world is called *atmospheric noise* (not to be confused with the noise produced by atmospheric absorption, as mentioned previously). The spectrum of atmospheric noise falls off rapidly with increasing frequency and is usually of little consequence above 50 MHz. It is seldom, therefore, an important consideration in radar design; except possibly for radars in the lower portion of the VHF region.

Anthropogenic Noise In preparing the previous (second) edition of this text, the publisher reminded me on several occasions to avoid the use of sexist terminology. I believe I was successful in doing so, except for one term: that of *man-made noise.* My reason for wanting to continue to use it was not that men usually make such noise (which they do), but I could not find a suitable substitute. Terms such as "human-made noise," "people-made noise," or "population-made noise" might be nonsexist, but they just didn't sound right. The publisher took pity on my inability to find a suitable substitute and relented; so on p. 463 of the 2d edition, the term "man-made noise" was allowed to appear. After the book was published, I came upon an excellent substitute, which is "anthropogenic noise." *Anthropogenic* is an adjective that means *relating to, or resulting from the influence of humans on nature.* It is a proper replacement for the no longer acceptable term *man-made noise.*

Electromagnetic emissions that appear as noise or interference to other electromagnetic services, originate from many possible sources: higher harmonics and other incidental radiation from transmitters, automobile ignition, electric razors, power tools, automatic garage door openers, fluorescent lights, industrial processing equipment, and power transmission lines.[96,97] Anthropogenic noise is more prevalent in urban and industrial areas than in rural areas. It decreases with increasing frequency and is seldom a factor in the design of microwave radars. It can be of concern, however, for VHF and lower-UHF

systems. Because of its variability in time and space, it is difficult to be precise about the quantitative nature of this form of noise. In the UHF radar frequency band, one source indicates[98] that the noise temperature of anthropogenic noise from a business region (industrial park, large shopping center, busy street, or highway) might be about 500 K, and for a residential region (at least two dwelling units per acre and no nearby highways) it might be about 200 K. At VHF and UHF, anthropogenic noise varies almost inversely as the cube of the frequency.

Interference and noise can also be experienced from other users of the electromagnetic spectrum, such as other radars and communications of all varieties. These sources of interference are generally different from anthropogenic noise, and is considered a problem in electromagnetic compatability (EMC).

Composite Graph Figure 8.19 is a composite graph of the several forms of environmental noise that might affect radar.[99] Only the minimum and maximum resultants from the various component factors are shown. Atmospheric noise and cosmic noise dominate at the lower frequencies, and atmospheric absorption noise dominates at the higher frequencies. The minimum noise levels occur from about 1 to 5 GHz (L to C band). Anthropogenic noise is not included on this graph since it is so variable and generally is of little consequence to radars that operate within the usual microwave radar bands. It can be quite important, however, for radars that operate at VHF or lower frequencies.

Earth Thermal-Noise The temperature of the earth is nominally 290 K; hence, it will radiate thermal noise. If an antenna beam illuminates the ground, it will receive a portion

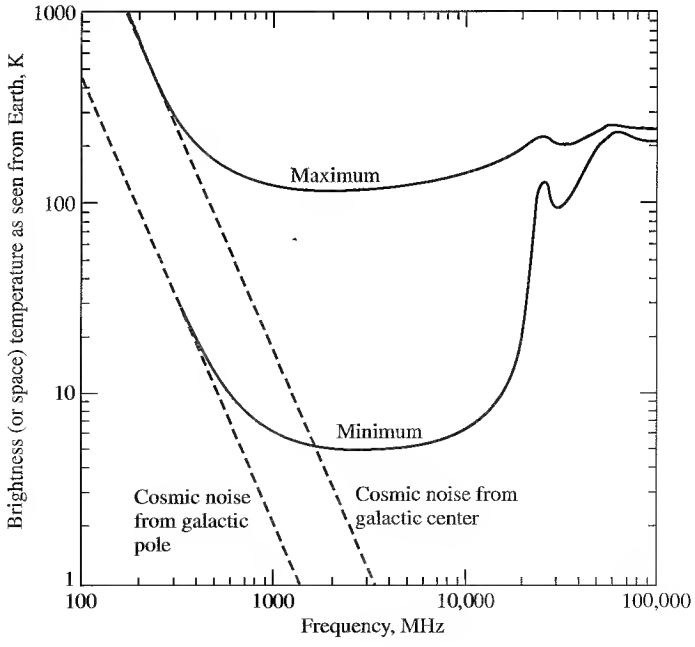

Figure 8.19 Maximum and minimum brightness temperatures of the sky as seen by an ideal single-polarizatian antenna an earth. (After Green and Lebenbaum.[99])

of the thermal noise radiated by the earth. The actual noise temperature seen by the receiver depends on whether the entire main beam of the antenna views the ground or if only a portion of the beam does so. The radiated noise depends on the emissivity of the ground as well as its temperature. Thus the brightness temperature seen by the antenna will be less than the actual temperature when the emissivity of the ground is less than unity, as will happen if the antenna views a water surface. The effect of the thermal noise radiation from the ground will affect only those systems with very sensitive receivers, generally those with noise figures of a fraction of a decibel. Radar receivers are seldom that sensitive; hence, the thermal noise radiated by the ground usually does not bother conventional radars.

8.9 OTHER PROPAGATION EFFECTS

Radar Siting Minimizing of environmental noise effects sometimes can be an important consideration in determining where a radar should be located. The siting of a radar also depends on the masking (obscuring or screening of targets) due to terrain and the backscatter from terrain features. It is especially important to know how the terrain affects the performance of ground-based radars when there is either severe masking, severe clutter echoes, or when low altitude targets have to be detected with high reliability.

The air-surveillance radars employed during World War II had no doppler processing, so that an aircraft target located in the same radar resolution cell as a clutter echo was likely to be undetected because of the large clutter echoes. As mentioned previously, when siting military air-surveillance radars at that time, it was desired that a site be chosen such that the surrounding terrain would shield clutter echoes from the radar. In effect, the terrain was used to mask the low-lying clutter echo and prevent it from entering the radar receiver so that aircraft at high altitudes could be seen without the presence of clutter. That was satisfactory in World War II, since heavy bomber aircraft generally flew at high altitudes. Modern aircraft and missiles, however, fly at low altitudes to deliberately avoid a radar's coverage. The military radar designer can respond by siting the antenna as high as practical and employing doppler processing to separate moving targets from fixed clutter echoes. Thus the siting of ground-based military air-defense systems has to take account of the local terrain so as to minimize the regions where the detection ranges of low-altitude targets are significantly reduced because of terrain masking.

The effect of terrain is an important part of the siting of civil air-traffic control radars. Computer software has been developed for providing detailed information about the terrain and its effect on civil air-traffic control radars so that the performance of a potential radar site can be determined before the radar is installed.[100] This program, called the Radar Support System (RSS), provides information that allows the radar designer to optimize the performance of a site-specific sensor by selecting the optimum radar height, optimum beam-tilt-angle, sensitivity time control (STC) characteristics, and to determine the likelihood of false alarms due to echoes from highway traffic or large clutter echoes. The input to RSS includes a digital model of the terrain obtained from databases available from the United States Geological Survey (USGS) or the Defense Mapping Agency. The height resolution is one meter and the steps in latitude and longitude are three seconds. There is

also a USGS database of land use and land cover with the same latitude/longitude quantization. It identifies the land as one of ten possibilities; such as urban, agricultural, forest, wet land, barren land, and so forth. Also included is a cultural database that provides three-dimensional models of the significant buildings near the radar site (such as an airport), and includes an estimate of the construction material of each structure. The RSS determines plots of the line-of-sight visibility from the radar, areas which are screened from the radar, the radar cross section of all visible terrain cells, and the probability of detection for specified targets.

Similar computer models and terrain databases have been applied to a military overland situation when the radar is located off shore.[101] Based on the Defense Mapping Agency's Digital Terrain Elevation Data and propagation programs like those mentioned in the previous section for standard and nonstandard atmospheric refraction conditions, it determines terrain and target visibility, masking, clutter echo strength, and plots the results on a maplike presentation to show how radar coverage is affected by the environment.

Atmospheric Lens-Effect Loss Weil[102,103] has shown there is another effect of atmospheric refraction on radar propagation, in addition to what was discussed in Secs. 8.4 and 8.5. The variation of standard refractivity with altitude causes the atmosphere to act as a negative lens that decreases the radiated energy density incident on a target. This loss is independent of radar frequency. Unlike atmospheric attenuation, the lens-effect loss continues to increase at ranges beyond the sensible atmosphere, but it approaches a limiting value asymptotically. For a CRPL exponential atmosphere with surface refractivity equal to 313, the loss is less than 1 dB at a range of 200 nmi and 0° elevation angle, and less than 0.18 dB at an elevation angle of 5°. The limiting values at very long range (10,000 nmi) are 2.9 dB at 0° elevation and 0.27 dB at 5° elevation. The lens-effect loss is an additional loss that is additive to the atmospheric attenuation. It is usually small enough to be neglected, except at low elevation angles and long range.

Ionospheric Propagation at Microwave Frequencies The ionosphere is a partially ionized region of the upper atmosphere that extends from about 50 km to 2000 km in altitude.[104] It is generated by high-energy particles that travel from the sun to ionize the atoms of the thin upper atmosphere. The refraction, or bending, of electromagnetic radiation by the ionosphere allows long-range propagation by shortwaves (the HF region) that is well know to radio amateurs. It is also the basis for HF over-the-horizon radar which allows the detection of aircraft, ships, and ballistic missiles at ranges extending out to 2000 nmi and beyond. The ionosphere is usually considered transparent to microwave radiation, but this is not fully correct. It can adversely affect in several ways the propagation of microwave radiation that travels through it.

Faraday Rotation of Polarization An electromagnetic wave experiences a rotation of its plane of polarization when traveling in an ionized medium (the ionosphere) and a magnetic field (that of the earth). This is known as *Faraday rotation.* If a ground-based radar is to detect satellites and other space objects, and if the radar employs linear polarization, the polarization of the echo signal will be different from that transmitted. A loss in signal can result. If, for example, the polarization were rotated by 90° because of

Faraday rotation, the received signal would be zero since the polarization is orthogonal to that of the transmitting antenna (which is assumed to be the same antenna as that used for receiving). The amount of polarization rotation varies inversely as f^2, where f = radar frequency. The rotation is determined by the total electron content of the ionosphere seen over the radar propagation path, which depends on the radar location, time of day, time of year, and the sunspot cycle. The effect is greater when the radar beam is pointing north or south and minimum when pointing east or west (directions are relative to magnetic north).

Radars for the detection of extraterrestrial targets that operate at UHF or lower frequencies can encounter loss due to the large polarization rotations of their echo signals. One solution for radars that are subject to Faraday rotation is to transmit on a single linear polarization (for example, vertical) and receive on two orthogonal linear polarizations (horizontal and vertical) in order to avoid loss in signal because of Faraday rotation. The echo signals in each polarization receive-channel are processed separately and then combined. This technique has been used in UHF radars for the detection of space objects such as BMEWS (ballistic missile early warning system), the AN/FPS-85 space surveillance radar, and the Pave Paws missile warning radar. At one time it was thought that radars at L band did not experience sufficient polarization rotation to require receiving with dual polarizations. Faraday rotation, however, can sometimes be significant enough at L band to require compensation.[105] The maximum one-way polarization rotation at a frequency of 1 GHz, for example, has been said to be 108° for a radar in the United States that views a target at an elevation angle of 30°.[106] Faraday rotation can also affect spaceborne radars viewing ground targets.

Other Ionospheric Effects The ionosphere will introduce a time delay that is inversely proportional to f^2. At 1 GHz, the maximum delay is said to be 0.25 μs.[105] There can also be refraction of the beam, loss by absorption, and frequency dispersion that introduces distortion into wideband signals. These effects are generally small at microwave frequencies for most radar applications that propagate through the ionosphere. There is one important example, however, where compensation had to be made in a microwave radar to avoid degradation of performance because of dispersion when propagating through the ionosphere. This occurred for the Cobra Dane high resolution L-band radar (1175 to 1375 MHz).[107]

The Cobra Dane radar, located on the island of Shemya at the southern tip of the Aleutian island chain in Alaska, was designed to gather intelligence information on Soviet ballistic missile systems. Its high range-resolution waveform employed a 1000-μs linear FM pulse with a 200-MHz bandwidth. Stretch pulse compression was incorporated to achieve a range resolution of about one meter. The time delay in propagating through the ionosphere was different at the low-frequency end of the 200-MHz bandwidth compared with the time delay at the high end of the bandwidth. This difference in propagation time was sufficient to introduce phase distortion and broaden the compressed pulse width unless compensated. The necessary corrections were obtained by predistorting the transmitted pulse by the inverse of the distortions introduced by the ionosphere. In addition to the ionospheric corrections, there had to be a correction applied to account for the fact that the doppler-frequency shift also was not constant over the 200-MHz bandwidth of the high-resolution waveform.

REFERENCES

1. Bachynski, M. P. "Microwave Propagation Over Rough Surfaces." *RCA Review,* 20, no. 2 (June 1959), pp. 308–335.
2. Ament, W. S. "Toward a Theory of Reflection by a Rough Surface." *Proc. IRE,* vol. 41 (January 1953), pp. 142–146.
3. Beard, C. I. "Coherent and Incoherent Scattering of Microwaves from the Ocean." *IRE Trans.* AP-9 (September 1961), pp. 470–483.
4. Miller, A. R., R. M. Brown, and E. Vegh. "New Derivation for the Rough-Surface Reflection Coefficient and the Distribution of Sea-Wave Elevations." *IEE Proc.,* 131, Pt. H (1984), pp. 114–116.
5. Miller, A. R., and E. Vegh. "Family of Curves for the Rough Surface Reflection Coefficient." *IEE Proc.* 133, Pt. H (December 1986), pp. 483–489.
6. Barton, D. K. "Low-Angle Radar Tracking." *Proc. IEEE* 62 (June 1974), pp. 687–704.
7. Miller, A. R., and E. Vegh. "Exact Result for the Grazing Angle of Specular Reflection from a Sphere." Naval Research Laboratory, Washington, D.C., Memorandum Rep. 6867, August 9, 1991.
8. Burrows, C. R., and S. S. Attwood. *Radio Wave Propagation.* New York: Academic, 1949.
9. Shibuya, S. *A Basic Atlas of Radio-Wave Propagation.* New York: John Wiley, 1987.
10. Blake, L. "Machine Plotting of Radio/Radar Vertical-Plane Coverage Diagrams." Naval Research Laboratory, Washington, D.C. Rep. 7098, June 25, 1970 (AD 709897).
11. Skolnik, M. "Improvements for Air-Surveillance Radar." *Proc. 1999 IEEE Radar Conf.* pp. 18–21, IEEE Catalog no. 99CH36249.
12. ITU-R Recommendation P.453–5, "The Radio Refractive Index: Its Formula and Refractivity Data," 1995.
13. Hitney, H. V. "Refractive Effects from VHF to EHF, Part A: Propagation Mechanisms." Paper no. 4A in *Propagation Modeling and Decision Aids for Communications, Radar, and Navigation Systems.* AGARD-LS-196, NATO, September 1994.
14. Bean, B. R., and E. J. Dutton. "Radio Meteorology," National Bureau of Standards Monograph 92, March 1, 1966.
15. Shibuya, S. Ref. 9, p. 28.
16. Bean and Dutton. Ref. 14, Secs. 3.1 and 3.2.
17. Bean, B. R. "The Geographical and Height Distribution of the Gradient of Refractive Index." *Proc. IRE,* 41 (April 1953), pp. 549–550.
18. Bean, B. R. et al. "A World Atlas of Atmospheric Radio Refractivity," U. S. Dept. of Commerce, ESSA Monograph 1, 1966.

19. Hall, M. P. M., L. W. Barclay, and M. T. Hewitt. *Propagation of Radiowaves.* London: Institution of Electrical Engineers, 1996, Sec. 6.2.

20. Blake, L. V. "Prediction of Radar Range." *Radar Handbook,* 2nd ed. M. Skolnik (Ed.). New York: McGraw-Hill, 1990, Chap. 2, Fig. 2.18.

21. Tank, W. G. "Atmospheric Effects." *Airborne Early Warning.* W. C. Morchin (Ed.). Boston, MA: Artech House, 1990, Chap. 3. See also Morchin, W. *Radar Engineer's Sourcebook.* Boston, MA: Artech House, 1993, Sec. 15.4.3.

22. Bauer, K. W. "Range-Height-Angle Charts with Lookdown Capability." *Microwave J.* 24 (October 1981), pp. 89–92.

23. Jursa, A. S. (Ed.). *Handbook of Geophysics and the Space Environment.* U.S. Air Force Geophysics Laboratory, 1985. (Available from National Technical Information Service, Springfield, VA, 22161.)

24. Valley, S. L., (Ed). *Handbook of Geophysics and Space Environments.* New York: McGraw-Hill, 1965.

25. Shannon, H. H. "Recent Refraction Data Corrects Radar Errors." *Electronics* 35, no. 49 (Dec. 7, 1962), pp. 52–56.

26. Blake, L. V. "Ray Height Computation for a Continuous Nonlinear Atmospheric Refractive-Index Profile." *Radio Science* 3 (January 1968), pp. 85–92.

27. Brown, B. P. "Radar Height Finding." *Radar Handbook,* 1st ed., M. Skolnik (Ed.). New York: McGraw-Hill, 1970, Chap. 22, Sec. 22.3.

28. Murrow, D. J. "Height Finding and 3D Radar." In *Radar Handbook,* 2nd ed. M. Skolnik (Ed.). New York: McGraw-Hill, 1990, Chap. 20, Sec. 20.2.

29. Barnett, K. M., and S. H. Brown. "Accuracy of Calculated Radar Refraction Errors." *IEEE Trans.* AP-13 (November 1965), p. 986.

30. Nathanson, F. E. *Radar Design Principles,* 2nd ed. New York: McGraw-Hill, 1991, Fig. 6.26.

31. Robertshaw, G. "How Accurate is Range Correction?" *Microwaves & RF* 25 (March 1986), pp. 129–132.

32. Rowland, J. R., and S. M. Babin. "Fine-Scale Measurements of Microwave Refractivity Profiles with Helicopter and Low-Cost Rocket Probes." *Johns Hopkins APL Tech. Dig* 8, no. 4 (1987), pp. 413–417.

33. Bean, B. R., and E. J. Dutton. Ref. 13, Sec. 2.3.

34. Anderson, L. J., and E. E. Gossard. "Prediction of Oceanic Duct Propagation from Climatological Data." *IRE Trans.* AP-3 (October 1955), pp. 163–167.

35. Anderson, K. D. "Radar Measurements at 16.5 GHz in the Oceanic Evaporation Duct." *IEEE Trans.*. AP-37 (January 1989), pp. 100–106.

36. Katzin, M., R. W. Bauchman, and W. Binnian. "3- and 9-Centimeter Propagation in Low Ocean Ducts." *Proc. IRE* 35 (September 1947), pp. 891–905.

37. Jeske, H. "State and Limits of Prediction Methods of Radar Wave Propagation Conditions Over the Sea." In *Modern Topics in Microwave Propagation and Air-Sea Interaction,* A. Zancla (Ed.). D. Reidel Publishing, 1973.

38. Patterson, W. L., et al. "Engineer's Refractive Effects Prediction System (EREPS)." Version 3.0, Naval Command, Control, and Ocean Surveillance Center, RDT&E Division, San Diego, CA, Tech. Document 2648, May, 1994.

39. Paulus, R. A. "Practical Applications of an Evaporation Duct Model." *Radio Science* 20 (July–August 1985), pp. 887–896.

40. Jeske, H. "The State of Radar-Range Prediction Over Sea." *AGARD Conf. Proceedings* 70(2) (1971), pp. 50.1–50.10.

41. Hitney, H. V., A. E. Barrios, and G. E. Lindem. "Engineer's Refractive Effects Prediction System (EREPS) User's Manual." Naval Ocean Systems Center, San Diego, CA, July 1988, (AD 203443)

42. Babin, S. M., G. S. Young, and J. A. Carton. "A New Model for the Oceanic Evaporation Duct." *J. Applied Meteorology* 36 (March 1997), pp. 193–204.

43. Anderson, K. D. "94-GHz Propagation in the Evaporation Duct." *IEEE Trans.* AP-38 (May 1990), pp. 746–753.

44. Joseph, R. I., and G. D. Smith. "Propagation in an Evaporation Duct: Results in Some Simple Analytic Models." *Radio Science* 7 (April 1972), pp. 433–441.

45. Früchtenicht, H. W. "Notes on Duct Influences on Line-of-Sight Propagation." *IEEE Trans.* AP-22 (March 1974), pp. 295–302.

46. Giger, A. J. *Low-Angle Microwave Propagation.* Norwood, MA: Artech House, 1991, Sec. 2.5.

47. Anderson, K. D. "Radar Detection of Low-Altitude Targets in a Maritime Environment." *IEEE Trans.* AP-43 (June 1995), pp. 609–613.

48. Hitney, H. V. Ref. 13, Sec. 6.2.

49. Patterson, W. L., et al. Ref. 38, pp. 12–14.

50. Battan, L. J. *Radar Observation of the Atmosphere.* Chicago: University of Chicago Press, 1973.

51. Pappert, R. A., and C. L. Goodhart. "A Numerical Study of Tropospheric Ducting at HF." *Radio Science* 14 (September–October 1979), pp. 803–813.

52. Appreciation is expressed to John Walters of the U. S. Naval Research Laboratory for supplying this information, and to Vilhelm Gregers-Hansen who originally created the figure.

53. Ringwalt, D. L., and F. C. McDonald. "Elevated Duct Propagation in the Tradewinds." *IRE Trans.* AP-9 (July 1961), pp. 377–383.

54. Guinard, N. W., J. Ransone, D. Randall, C. Purves, and P. Watkins. "Propagation Through an Elevated Duct: Tradewinds III." *IEEE Trans.* AP-12 (July 1964), pp. 479–490.

55. Purves, C. G. "Geophysical Aspects of Atmospheric Refraction." Naval Research Laboratory, Washington, D.C. Rep. 7725, June 7, 1974.

56. Hitney, H. V., R. A. Pappert, C. P. Hattan, and C. L. Goodhart. "Evaporation Duct Influences on Beyond-the-Horizon High Altitude Signals." *Radio Science* 13 (July–August 1978), pp. 669–675.

57. Kerr, D. E. (Ed.). *Propagation of Short Radio Waves.* MIT Radiation Laboratory Series, vol. 13 New York: McGraw-Hill, 1951.

58. Brookner, E., E. Ferraro, and G. D. Ouderkirk. "Radar Performance During Propagation Fades in the Mid-Atlantic Region." *IEEE Trans.* AP-46 (July 1998), pp. 1056–1064.

59. Day, J. P., and L. G. Trolese. "Propagation of Short Radio Waves Over Desert Terrain." *Proc. IRE* 38 (February 1950), pp. 165–175.

60. Donohue, D. J., and J. R. Kuttler. "Modeling Radar Propagation Over Terrain." *Johns Hopkins APL Tech. Dig.* 18, no. 2 (1997), pp. 279–287.

61. Dockery, G. D. "Method of Modeling Sea Surface Clutter in Complicated Propagation Environments." *IEE Proc.* 137, no. 2, Pt. F (April 1990), pp. 73–79.

62. Reilly, J. P., and G. D. Dockery. "Influence of Evaporation Ducts on Radar Sea Return." *IEE Proc.* 137, no. 2, Pt. F (April 1990), pp. 80–88.

63. Heimken, H. F. "Low-Grazing-Angle Radar Backscatter from the Ocean Surface." *IEE Proc.* 137, no. 2, Pt. 7 (April 1990), pp. 113–117.

64. Booker, H. G. "Elements of Radar Meteorology: How Weather and Climate Cause Unorthodox Radar Vision Beyond the Geometrical Horizon." *J. IEE* 93, Pt. IIIA (1946), pp. 69–78.

65. Nathanson, F. E. Ref. 30, Sec. 9.5.

66. Hitney, H. V. "Refractive Effects from VHF to EHF, Part B: Propagation Models." Paper no. 4B in *Propagation Modeling and Decision Aids for Communications, Radar, and Navigation Systems.* AGARD-LS-196, NATO, September 1994.

67. Kerr, D. E. Ref. 57.

68. Budden, K. G. *The Wave-Guide Mode Theory of Wave Propagation.* Englewood Cliffs, NJ: Prentice-Hall, 1961.

69. Dockery, G. D. "Modeling Electromagnetic Wave Propagation in the Troposphere Using the Parabolic Equation." *IEEE Trans.* AP-36 (October 1988), pp. 1464–1470.

70. McArthur, R. J. "Propagation Modeling Over Irregular Terrain Using the Split-Step Parabolic Equation Method." *International Conf. Radar 92, IEE Conf. Publication 365,* London, 1992, pp. 54–57.

71. Barrios, A. E. "Parabolic Equation Modeling in Horizontally Inhomogeneous Environments." *IEEE Trans.* AP-40 (July 1992), pp. 791–797.

72. Barrios, A. E. "A Terrain Parabolic Equation Model for Propagation in the Troposphere." *IEEE Trans.* AP-42 (January 1994), pp. 90–98.

73. Hitney. H. V. "Hybrid Ray Optics and Parabolic Equations Methods for Radar Propagation Modeling." *Int. Conf. Radar 92, IEE Conf. Publication 365,* London (1992), pp. 58–61.

74. Richter, J. H. "Electromagnetic Wave Propagation Assessment." *AGARD Highlights* 92/1 (March 1992), pp. 6–14.

75. Hitney, H. V., and J. H. Richter. "Integrated Refractive Effects Prediction System (IREPS)." *Naval Engineers J.* 2 (April 1976), pp. 257–262.

76. Patterson, W.L., et al. *IREPS 3.0 User's Manual.* Naval Ocean Systems Center (NOSC), San Diego, CA, Tech. Document 1151, September 1987. See also Revision PC-2.0, Tech. Document 1874, August 1990.

77. Patterson, W. L. *Advanced Refractive Effects Prediction Sysem (AREPS), Version 1.0 User's Manual.* SPAWAR Systems Center, San Diego, Technical Document 3028, April 1998.

78. Gelsenheyner, S. "Computerized Data Help Predict Anomalous Propagation." *Microwave System News* 11 (April 1982), pp. 45–46.

79. Belobrova, M. V., et al. "Software Suite for Diagnosing USW Propagation Over the Sea." *Radiophysics and Quantum Electronics* 33 (June 1991), pp. 961–965.

80. Skolnik, M. I. "Radar Horizon and Propagation Loss." *Proc. IRE* 45 (May 1957), pp. 697–698.

81. Millman, G. H., and G. R. Nelson. "Surface Wave HF Radar for Over-the-Horizon Detection." *Record of the IEEE 1980 International Radar Conf.* pp. 106–112, IEEE Publication 80CH1493–6 AES, New York.

82. Powers, R. L., L. M. Lewandoski, and R. J. Dinger. "High Frequency Surface Wave Radar—HFSWR." *Sea Technology* 37 (November 1996), pp. 25–32.

83. Headrick, J.M., and M. I. Skolnik. "Over-the-Horizon Radar in the HF Band." *Proc. IEEE* 62 (June 1974), pp. 664–673.

84. Lipa, B. J., and D. E. Barrick. "Extraction of Sea State from HF Radar Sea Echo: Mathematical Theory and Modeling." *Radio Science* 21 (January–February 1986), pp. 81–100.

85. Lipa, B. J., D. E. Barrick, J. Isaacson, and P. M. Lilleboe. "CODAR Wave Measurements From a North Sea Semisubmersible." *IEEE J. Oceanic Engineering* 15 (April 1990), pp. 119–125.

86. Graber, H. C., B. K. Haus, R. D. Chapman, and L. N. Shay. "HF Radar Comparisons with Moored Estimates of Current Speed and Direction: Expected Differences and Implications." *J. Geophys. Res.* 102, no. C8 (August 15, 1997), pp. 18,749–18,766.

87. Walsh, J., B. J. Dawe, and S. K. Srivastava. "Remote Sensing of Iceburgs by Ground-Wave Doppler Radar." *IEEE J. Oceanic Engineering* OE-11 (April 1986), 276–284.

88. Srivastava, S. K., and J. Walsh. "Over-the-Horizon Radar." Chapter 7 in *Remote Sensing of Sea Ice and Ice Bergs,* S. Haykin, E. O. Lewis, R. K. Raney, and J. R. Rossiter (Eds.). New York: John Wiley, 1994.

89. Straiton, A. W., and W. Tolbert. "Anomalies in the Absorption of Radio Waves by Atmospheric Gases." *Proc. IRE* 48 (May 1960), pp. 898–903.

90. Straiton, A. W. "The Absorption and Reradiation of Radio Waves by Oxygen and Water Vapor in the Atmosphere." *IEEE Trans.* AP-23 (July 1975), pp. 595–597.

91. Blake, L. V. "Prediction of Radar Range." In *Radar Handbook,* 1st ed. M. Skolnik (Ed.). New York: McGraw-Hill, 1970, Chap. 2, Sec. 2.7.

92. Baars, J. W. M. "The Measurement of Large Antennas with Cosmic Radio Sources." *IEEE Trans.* AP-21 (July 1973), pp. 461–474.

93. Graf, W., R. N. Bracewell, J. H. Deueter, and J. S. Rutherford. "The Sun as a Test Source for Boresight Calibration of Microwave Antennas." *IEEE Trans.* AP-19 (September 1971), pp. 606–612.

94. Evans, G. E. *Antenna Measurement Techniques.* Boston, MA: Artech House, 1990, Secs. 2.6 and 3.3.3.

95. Schonland, B. F. J. *The Flight of Thunderbolts.* 2nd ed. Oxford, London: Clarendon Press, 1964.

96. Skomal, E. N. "Man-Made Noise in the M/W Frequency Range." *Microwave J.* 18 (January 1975), pp. 44–47.

97. Skomal, E. N. *Man-Made Radio Noise.* New York: Van Nostrand, 1978.

98. Ralston, J., J. Heagy, and R. Sullivan. "Environmental/Noise Effects on VHF/UHF UWB SAR." Institute for Defense Analyses, Alexandria, VA, IDA Paper, P-3385, September 1998.

99. Greene, J. C., and M. T. Lebenbaum. Letter in *Microwave J.* 2 (October 1959), pp. 13–14.

100. Pieramico, A. F., D. A. Rugger, and L. R. Moyer. "The Radar Support System (RSS): A Tool for Siting Radars and Predicting their Performance." *ATC Systems* 2, no. 1 (January/February 1996), pp. 32–40.

101. Lin, C. C., and J. P. Reilly. "A Site-Specific Model of Radar Terrain Backscatter and Shadowing." *Johns Hopkins APL Tech. Digest* 18, no. 3 (July–September 1997), pp. 432–447.

102. Weil, T. A. "Atmospheric Lens Effect; Another Loss for the Radar Range Equation." *IEEE Trans.* AES-9 (January 1973), pp. 51–54.

103. Shrader, W. W., and T. A. Weil. "Lens-Effect Loss for Distributed Targets." *IEEE Trans.* AES-23 (July 1987), pp. 594–595.

104. Goodman, J. M., and J. Aarons. "Ionospheric Effects on Modern Electronic Systems." *Proc. IEEE* 78 (March 1990), pp. 512–528.

105. Brookner, E., Hall, W. M., and R. H. Westlake. "Faraday Loss for L-band Radar and Communcations Systems." *IEEE Trans.* AES-21 (July 1985), pp. 459–469.

106. Flock, W. L. "Propagation Effects on Satellite Systems at Frequencies Below 10 GHz." *NASA Reference Publication 1108* (December 1983), Sec. 2.4.

107. Filer, E., and J. Hartt. "Cobra Dane Wideband Pulse Compression System." *IEEE EASCON '76,* pp. 61-A to 61-M.

PROBLEMS

8.1 In this problem, you may assume a flat earth. (a) What are the elevation angles (in degrees) of the two lowest elevation-pattern multipath interference lobes for an *L*-band (1300 MHz) radar antenna located at a height 50 ft above a perfectly conducting flat surface? (b) What is the height (in meters) of the peak of the first (lowest) lobe above the earth's surface at a range of 3 nmi? (c) Repeat (a) and (b) for an *X*-band (9375 MHz) radar antenna. (d) What can you conclude from the above about the detection of low-altitude targets and radar frequency? (e) When might the *X*-band ship navigation-radar of part (c) have trouble detecting navigation buoys because of multipath lobing, especially if the ship is sailing in calm waters? (You may assume that the echo from the buoy is due to a corner reflector mounted at the top of the buoy 6 m above mean sea level.)

8.2 Under what conditions might the received echo-signal power from a point target located over a flat conducting surface (such as a smooth sea) vary inversely as the eighth power of the range?

8.3 Figure 8.1 illustrates the two paths between the radar and a point target (the direct path and the surface-reflected path). Assume a radar transmits a single short-pulse with pulse duration much less than the time difference between the signals transiting these two paths; i. e., the pulse width is small compared to $2\Delta/c$, where Δ was given by Eq. (8.4). (You may think of the pulse as a delta function that propagates in space.) (a) Sketch the nature of the echo signal received back at the radar after reflection by the point target. (There will be more than one echo returned to the radar.) (b) Derive an expression for the time separation between the pulses? (c) How can this type of short-pulse transmission be used to measure the height of a target?

8.4 The lobes in the elevation pattern due to multipath (such as in Fig. 8.6b) cause loss of target signal when the target is within the null regions of the pattern. What might the radar system designer do to avoid the loss of signal due to the multipath nulls?

8.5 Many air-surveillance radars operate with the antenna beam pointed slightly upward so that the lower half-power point of the elevation pattern is directed along the horizon rather than have the maximum antenna gain along the horizon. Discuss the pros and cons of having the antenna half-power point at the horizon instead of the maximum antenna gain at the horizon.

8.6 What radar characteristics are important for detecting targets at low altitudes?

8.7 The caption of Fig. 8.6b states that this is a plot of the elevation pattern of a 900-MHz radar at an antenna height of 75 ft. Using Eq. (8.8) verify that this is correct based on the antenna pattern shown in Fig. 8.6b. Assume a flat earth and an effective earth's radius of 4/3. (Use of the lowest lobe, however, will probably not give as correct an answer as will the next higher lobe.)

8.8 (a) Show that the distance d to the horizon from a radar at a height h above a spherical earth of effective radius ka is $d = \sqrt{2kah}$. (b) If $k = 4/3$ and the actual radius of the earth $a = 3440$ nmi, what is the distance in nautical miles to the horizon for a radar at a height of 10,000 ft? (c) How much would the distance to the horizon in (b) be increased if the

atmospheric refraction were such that $k = 1.8$ instead of 1.33? (d) If a radar had a free-space range exactly equal to the distance to the horizon, d, why might it not be able to see a target located at the horizon?

8.9 The factor k that describes the modification to the earth's radius to account for atmospheric refraction was given by Eq. (8.16) as

$$k = \frac{1}{1 + a(dn/dh)}$$

where a = radius of the earth and dn/dh is the rate of change of the index of refraction with height. (a) What value of dn/dh results in $k = \infty$? (b) What does it mean when $k = \infty$?

8.10 In Sec. 8.4 of the text it is reported[25] that the range error due to atmospheric refraction is 97.5 ft for a target at 40,000 ft and an elevation angle of 3°. Compare this to the answer you get for the range error when using Eq. (8.19), based on different experimental data. (You might need to use Fig. 8.9. Take the surface refractivity to be 313.)

8.11 (a) Why are radars seldom operated at or near a frequency of 22 GHz or near 60 GHz? (b) What is the two-way attenuation of a radar signal (in dB) in the clear atmosphere at a frequency of 5 GHz when propagating 200 nmi (and back) at an elevation of 0°? (c) What is the two-way attenuation when the elevation angle is increased to 5°? (d) Why are aircraft targets not likely to be detected at long range at zero degrees elevation angle?

8.12 A shipboard military radar for detecting low-altitude missile targets over water might be based on either (1) microwave ducted propagation or (2) HF surface-wave propagation to extend the detection range beyond the horizon. Compare these two radar methods with respect to their effectiveness in performing this task. Include in your comparison the effect of their relative size, reliability for detection under all conditions, accuracy, and anything else you think is appropriate.

8.13 Equation 8.11b assumes that the antenna gain remains constant with frequency (which means the beamwidths remain constant), so the received echo signal power P_r varies as λ^{-2}, where λ = wavelength. How would the echo signal power P_r vary with wavelength if the antenna aperture A_e remained constant with frequency?